

Modeling natural attenuation of petroleum contaminants in aquifers: conceptual model and simulations

P. AAGAARD, Z. ZHENG AND G. BREEDVELD

Dep. of Geology, University of Oslo, 0316 Oslo, Norway
(aagaard@geologi.uio.no)

Lawrence Berkeley National Laboratory, Berkeley, CA 94720,
USA (zzuoping@lbl.gov)

Norwegian Geotechnical Institute, 0806 Oslo, Norway
(gbr@ngi.no)

Introduction

Natural attenuation of petroleum contaminants is often observed through biologically mediated transformation reactions using different electron acceptors. This leads to changes in geochemical conditions and induces mineral precipitation/dissolution reactions in groundwater environment. Reactive transport modeling, thus requires a coupling of biodegradation, geochemical reactions and transport. We have applied the one-dimensional transport in PHREEQC with user-specified kinetic formulation of dual Monod kinetics.

Conceptual model

We have adopted the dual Monod kinetics to describe growth and metabolism of microorganisms as a function of substrate, electron acceptors and nutrients. The Monod expression is conservative and rely on a minimum number of model parameters. We assumed a diverse microbial population able to degrade under various TEAPs, and adopted the Monod parameters from Essaid et al. (1995).

Simulations

Simulations of several laboratory (batch and column) biodegradation experiments and one field case (Zheng, 2001; Hunkeler et al., 1998) have been performed. The initial biomass showed an expected scale dependency, while the Monod parameters were kept constant except for minor adjustments. For Hunkeler's experiments all the major C-t-x observations were well simulated in addition to quantification of corresponding mineral dissolution and precipitation reactions.

Conclusions

PHREEQC reactive flow simulations with dual Monod kinetics included, represent an attractive approach to evaluate the degradation potential for contaminated aquifers.

References

- Essaid H.I., Bekins B.A., Godsy E.M. and Warren E. (1995) *Water Resour. Res.* **31**, 3309-3327
Hunkeler D., Jorger D., Haberli K., Hohener P. and Zeyer J. (1998) *J. Contam. Hydrol.* **32**, 41-61
Zheng Z. (2001) *Ph.D. thesis, University of Oslo*, 137p

A mixed proto-atmosphere during the runaway accretion

YUTAKA ABE, HIDENORI GENDA AND KENJI NISHIKAWA

Department of the Earth and Planetary Science, University of Tokyo, 7-3-1 Hongo, Bonkyo, Tokyo 113-33, JAPAN.
ayutaka@eps.s.u-tokyo.ac.jp

The surface environment of the Earth during its formation is reconstructed in accordance with a recent planetary formation theory. The recent planetary formation theory suggests two stages of planetary formation; the stage of runaway growth (e.g., Kokubo and Ida, 1998) followed by the stage of giant impacts (e.g., Chambers and Wetherill, 1998).

A Mars-sized planet forms in 10^6 years at the stage of the runaway growth. Since the solar nebula likely exists at this stage, the proto-Earth should have a distended solar-composition (H_2 -He) atmosphere (e.g., Hayashi et al, 1978) through gravitational attraction of the nebula gas. Also, impact degassing from Earth-forming planetesimals forms an atmosphere, which sometimes called as 'a steam atmosphere' (e.g., Abe and Matsui, 1986). Thus, a mixed proto-atmosphere composed of solar and degassed components would have formed. Though the structure of the mixed atmosphere embedded in the nebula gas is not well understood yet, it would be similar to that of the degassed atmosphere with an extended upper atmosphere. The proto-atmosphere would show a strong thermal blanketing effect, and a surface magma ocean is formed because of relatively frequent planetesimals impacts. Chemical interactions between the proto-atmosphere and the Earth's proto-mantle and core-materials proceed through the magma ocean. The formation of the mixed atmosphere and its chemical interaction during accretion has important effects on the budget of volatile components, in particular for the noble gas budget.

Though the solar nebula has likely been lost by the stage of giant impacts, the mixed proto-atmosphere would have survived the nebula dissipation, because the atmosphere is tightly bounded by the Earth's gravity field. This atmosphere should survive the stage of giant impacts with some modification (Genda and Abe, 2002).

References

- Abe, Y. and T. Matsui, 1986. *J. Geophys. Res.*, **91**, suppl., E291-E302.
Chambers, J. E., and G. W. Wetherill 1998. *Icarus* **136**, 304-327.
Hayashi, C., K. Nakazawa and H. Mizuno, 1979, *Earth Planet. Sci. Lett.*, **43**, 22-28.
Genda, h. and Y. Abe, in this volume.
Kokubo, E., and S. Ida 1998. *Icarus* **131**, 171-178.

The Pb isotope record of terrigenous input into the Tropical Atlantic

Wafa ABOUCHAMI¹ AND MATTHIAS ZABEL²

¹Max-Planck-Institut fuer Chemie, Postfach 3060, 55020

Mainz, Germany, wafa@mpch-mainz.mpg.de

²Dept of Geosciences, University of Bremen, Bremen, Germany

We report high-precision Pb isotope data on two sediments cores from the Equatorial Atlantic (GeoB1523-1 and GeoB2910-1) and show a synchronicity of Pb isotopic variations with glacial-interglacial cycles over the past 200 ka. Pb isotope data were obtained on bulk sediments. Holocene and LGM samples were leached in order to deconvolve the detrital and carbonate signals. The 200-ka Pb isotope record of the bulk sediments display periodic fluctuations in both cores. Despite distinct Pb isotopic signatures in the East and West Atlantic, both Pb isotope records follow the $\delta^{18}\text{O}$ record: interglacial periods are systematically more radiogenic than glacial periods. In Pb isotope space, the West Atlantic data form a unique Pb isotope array that is quite distinct from that of the East Atlantic where two trends are found. Leaching results show that in the West Atlantic, the carbonate fraction is less radiogenic than the residue and vice-versa in the East Atlantic. In both basins, however, the bulk sediment composition is shifted toward that of the residue, suggesting that the carbonates do not significantly contribute to the Pb budget of the bulk sediment. The Pb isotopic composition of the carbonates is different from that of ambient deep waters, as inferred from Fe-Mn crusts, and its significance remains to be determined.

We interpret the Pb isotopic differences between the East and West Atlantic as reflecting distinct terrigenous Pb sources. In the West, the terrigenous flux is overwhelmed by the Amazon discharge, while in the East, it is mostly derived from the Sahara-dust plume and nearby African terranes. The glacial-interglacial isotopic contrast along the Pb arrays is consistent with climate-dependent changes in the relative proportions of the contributing Pb source(s). The shift from radiogenic Pb during warm periods to unradiogenic Pb during cold periods suggests a strong coupling between the weathering style and its resulting products. The distinct Pb isotopic compositions of bulk sediments, residues and carbonates in the two cores show a complete decoupling of Pb sources in the two basins. The cyclicity of the bulk sediments Pb isotope records reflects variations in terrigenous fluxes into the Tropical Atlantic over the past ~200 ka and demonstrates a climate control on Pb inputs to the oceans.

Molecular and carbon isotopic characterization of polycyclic aromatic hydrocarbon distribution in mussels and associated sediments from the Massena-Cornwall area, St. Lawrence River

T. ABRAJANO, JR.¹, A. STARK⁻, J. SMITH², AND J HELLOU³

¹Department of Earth and Environmental Sciences, Rensselaer Polytechnic Institute, Troy, New York 12180 USA [abrajt@rpi.edu]

²Aquatic Ecosystems Protection Branch, National Water Research Institute, Burlington, ON B2Y 4A2 Canada

³Marine Chemistry Section Marine Environmental Sciences Division, Bedford Institute of Oceanography, Dartmouth, NS B2Y 4A2 Canada

This paper documents the molecular and compound-specific carbon isotope composition of polycyclic aromatic hydrocarbons (PAH) in mussels (of *L.l. radiata* and *E. complanata*) and associated sediments collected from the Massena and Cornwall areas of the St. Lawrence River. Scuba sampling of mussels with shell length 6.0 and 10.0 cm were performed in seven sites from the Massena and Cornwall sides of the River. Upon collection, the organisms were rinsed clean of sediment using river water, wrapped in pre-fired (550°C) hexane-rinsed aluminum foil, placed in freezer storage bags, and immediately frozen on dry ice. In the laboratory, the mussels were thawed for 30 min, opened, sexed, and shucked individually into acid-washed glass jars. Individual mussels were freeze-dried and five specimens from the same site, species, and sex were pooled for analysis. This composite sample was ground for 1 min in a Bel-Art Micro-Mill with stainless steel blades and grinding chamber. PAH extraction of mussel samples was performed by saponification of ground freeze-dried tissue. For each sample, saponification of ~10 g of sample was performed in 200 ml of 6 N KOH in a warm water bath (~35°C) for 24 hr in a darkened fume hood. After 24 hr, any remaining residue, usually < 0.25 g, was centrifuged off and washed with 5 x 10 ml of dichloromethane to recover the neutral fraction associated with the undigested residue. The digested portion was solvent exchanged with 5 x 100 ml of dichloromethane to recover the neutral fraction. All dichloromethane extracts were combined into a total neutral fraction and concentrated in a rotary evaporator at 35°C, dried under a stream of nitrogen, and stored at -20°C. Fused KOH was added to deionized water to make a 1 liter 6 N solution which was solvent extracted with 3 x 100 ml of dichloromethane to ensure purity. Sediment analyses were performed following Stark et al. (2002).

In all the sites examined, both parental and alkylated PAH were noted, with 4 to 5-ring parental species predominating in both the mussels and sediments. All mollusc samples contained notable amounts of DBT, methyl-DBT, phenyl-Na, the $m/z = 218$ amu compound, the $m/z = 226$ compound, and alkylated 3 and 4-ring species.

Unpacking “vital effects” in biogenic carbonates using deep-sea corals

JESS F. ADKINS

MS 100-23; Department of Geological and Planetary Sciences; Caltech, Pasadena, CA 91125 USA
(jess@gps.caltech.edu)

Offsets from isotopic equilibrium in biogenic carbonates have complicated paleoclimate reconstructions for decades. We use a new archive of climate, deep-sea corals, to evaluate the calcification processes, independent of photosynthesis, that contribute to these offsets. Carbon and oxygen stable isotope data from six modern deep-sea corals show strong linear trends between $\delta^{13}\text{C}$ and $\delta^{18}\text{O}$. Slopes of these trends between samples are similar and range between 2.1-2.6 for $\Delta\delta^{13}\text{C}/\Delta\delta^{18}\text{O}$. Linear trends intersect isotopic equilibrium for $\delta^{18}\text{O}$ and are slightly depleted for $\delta^{13}\text{C}$. Variations in the isotopic ratios are strongly correlated with the density banding structure. Isotopically depleted aragonite is associated with light, fast precipitating bands, while isotopically enriched points correspond to slowly accumulating less dense aragonite. The densest, white band at the trabecular center is furthest from isotopic equilibrium for both carbon and oxygen. Data from this region fall off the linear trend between $\delta^{18}\text{O}$ and $\delta^{13}\text{C}$. This deviation, where $\delta^{13}\text{C}$ is anomalously heavy for the $\delta^{18}\text{O}$, does not support “vital effect” mechanisms that call upon kinetic fractionation to explain offsets from isotopic equilibrium. We propose a new mechanism for “vital effects” in biogenic carbonates that is based on a thermodynamic response to a biologically induced pH gradient in the calcifying region. We also present a numerical model of the calcifying region that can explain many of the observed features of stable isotope “vital effects” in a variety of marine organisms.

The temperature, salinity and $\delta^{18}\text{O}$ of the LGM deep ocean

JESS F. ADKINS¹, KATHERINE MCINTYRE¹ AND DANIEL P. SCHRAG²

¹ MS 100-23; Department of Geological and Planetary Sciences; Caltech; Pasadena, CA 91125 USA
(jess@gps.caltech.edu, kmci@gps.caltech.edu)

² Department of Earth and Planetary Sciences; Harvard University; 20 Oxford St.; Cambridge, MA 02138 USA
(schrag@eps.harvard.edu)

We have measured the sediment pore fluid profiles of $\delta^{18}\text{O}$ and chloride ion concentration at five ODP sites covering the North Atlantic, the Southern and the South Pacific oceans. Combining high precision data with samples at high depth resolution, we can constrain the amplitude and location of the pore water salinity and $\delta^{18}\text{O}$ maximum that results from glacial extension during the LGM. A 1-D diffusion/advection model, forced at the top boundary with the shape of the global sea level curve, allows us to reconstruct the size of bottom water change from LGM to today at each site. Combined with benthic foraminiferal $\delta^{18}\text{O}$ this data allows us to reconstruct the temperature, salinity and $\delta^{18}\text{O}$ of the LGM deep waters.

The resulting temperature versus salinity plot for the LGM shows several important features. First, outside of the shallow high latitude North Atlantic (site 981), all of our sites are within error of the seawater freezing point. Second, the Southern Ocean (site 1093) is the saltiest water in the LGM deep ocean, by over 1 psu compared to the deep North Atlantic (site 1063). Third, the mean salinity of the ocean, if our deep south Pacific site (1123) is representative of the mean ocean, is larger than the 35.8 psu implied by ~125 meters of global eustatic sea level change. This last point needs to be confirmed with cores from the deep equatorial and deep north Pacific ocean. The water $\delta^{18}\text{O}$ versus salinity plot indicates that the salty Southern Ocean deep waters were formed in large part by sea ice formation and export from the sinking region. Overall the LGM deep waters were at or near the freezing point and reversed from the modern salinity gradient in the Atlantic Ocean.

Excess air in groundwater as a proxy for paleo-humidity

W. AESCHBACH-HERTIG¹, U. BEYERLE², R. KIPFER^{1,3}

¹Water Resources and Drinking Water, EAWAG, CH-8600 Dübendorf, Switzerland (aeschbach@eawag.ch)

²Climate and Environmental Physics, University of Bern, CH-3012 Bern, Switzerland (beyerle@climate.unibe.ch)

³Isotope Geology, ETH Zürich, CH-8092 Zürich, Switzerland (kipfer@eawag.ch)

The concentrations of dissolved noble gases in groundwater usually exceed the atmospheric solubility equilibrium. The equilibrium component provides information on paleotemperatures via the temperature dependent solubilities. The excess component (“excess air”) might reflect other environmental conditions – in particular humidity – during groundwater recharge.

Excess air originates from air bubbles that are trapped in the quasi-saturated soil zone, i.e. the zone affected by periodic fluctuations of the groundwater table. Contrary to previous assumptions, this “entrapped air” is usually not completely dissolved. Instead, a new equilibrium between partially dissolved bubbles and groundwater is reached. Model calculations as well as laboratory experiments show that the size of the resulting gas excesses, e.g. the relative Ne excess ΔNe , is directly linked to the hydrostatic pressure on the entrapped gas bubbles.

The hydrostatic pressure in the quasi-saturated zone depends on the amplitude of water table fluctuations, which in turn reflects the intensity and variability of recharge. As a result, ΔNe is expected to be linked to the climate variable precipitation. This link appears to be particularly strong in semi-arid climate zones, where precipitation and recharge exhibit large seasonal and inter-annual fluctuations.

For example, in groundwater from the Continental Terminal aquifers of Niger, we found correlated variations of stable isotope ratios, excess air (ΔNe), and noble gas temperature (NGT) over the past 40 kyr. Compared to modern samples from the top aquifer, the late Pleistocene to mid Holocene samples from the deeper aquifers show depleted stable isotopes, higher values of ΔNe , and lower NGTs.

These observations consistently indicate recharge during more humid periods. In such periods with more intense rainfall, stable isotopes were depleted due to the amount effect, ΔNe was increased due to larger water table fluctuations, and NGTs were lowered by a reduction of the difference between soil and air temperature due to increased vegetation. In the case of Niger, it appears that excess air reflects groundwater recharge intensity, whereas NGT does not directly indicate atmospheric temperature.

Experimental Constraints on Core Formation

CARL B. AGEE

Institute of Meteoritics, Department of Earth and Planetary Sciences, University of New Mexico, Albuquerque NM, 87131, USA, agee@unm.edu

Over the past several years numerous high-pressure experimental studies have placed important constraints on the physics and chemistry of planetary core formation. For the Earth, core formation appears to have occurred within a deep magma ocean.

Dihedral angle measurements of metal/silicate wetting experiments show that core melt segregation from a solid silicate mantle, under static compression, is inefficient and excess metal would be stranded in the mantle. Efficient metal segregation, consistent with the observed upper mantle, may require significant silicate melting where liquid metal sinks to the core by rainfall. Experiments on wetting of perovskite suggest that percolation of metal melt is significantly more efficient in the lower mantle.

Moderately siderophile elements Ni and Co have metal/silicate partition coefficients that decrease with pressure and converge to a value consistent with the average Ni/Co of the Earth's upper mantle. This convergence of Ni and Co partition coefficients occurs in the range 28-35 GPa (750-900 km depth) and can be interpreted as the pressure or depth of the bottom of a magma ocean where the upper part of the mantle last equilibrated with sinking core melt.

Slightly siderophile elements V, Cr, and Mn are similarly depleted in the mantles of the Earth and Moon. New metal-silicate partitioning data for V, Cr, and Mn explain the mantle depletions by core formation at super-liquidus temperatures (>3000 C) under oxygen fugacity conditions more than two log units below the iron-wüstite buffer. The data do not require the mantle of the Moon to be derived from the Earth's mantle.

Light element metal/silicate partitioning studies show that sulfur's affinity for liquid metal increases strongly with pressure, while Si and O are highly lithophile at all experimental pressures using chondritic compositions at ~iron-wüstite buffer. Si and O content of the core should be strongly dependent on the oxygen fugacity in early Earth. Sulfur may be the dominant light element in the core if a sufficient quantity of it was sequestered in the Earth during accretion. Interestingly, the partitioning data indicate that the sulfur content of the upper mantle (250 ppm) is too high to have equilibrated with a molten outer core containing 2-10 wt% sulfur. Mass balance requires that additional sulfur be added to the upper mantle from other sources, possibly as part of a 0.2-0.6% Earth-mass late veneer.

Hf-Pb isotope systematics in MORB along the Reykjanes Ridge (50-64°N)

A. AGRANIER¹, J. Blichert-Toft¹, J.-G. Schilling²,
B. Nelson³ and F. Albarede¹

¹ Ecole Normale Supérieure, 46 allée d'Italie, 69364 Lyon
Cedex 7, France (arnaud.agranier@ens-lyon.fr)

² Graduate School of Oceanography, Narragansett Bay
Campus, University of Rhode Island, Narragansett, RI
02882-1197, USA

³ Department of Earth and Space Sciences, University of
Washington, Box 351310, Seattle, WA 98195, USA

To further elucidate interaction between the Iceland mantle plume and the Mid-Atlantic Ridge (MAR) with greater sampling density, coverage, and analytical precision, we report Hf and Pb isotope data for 56 basalt glasses from the Reykjanes Ridge (RR) covering its entire latitudinal extent from 64°N to 50°N. Hf and Pb were separated from the same leached sample dissolutions and measured for their isotopic compositions by MC-ICP-MS.

Overall, Hf and Pb isotope ratios display good negative correlations. Between 64°N and 61°N, both Hf and Pb isotope along-ridge variations confirm the major gradient previously established with fewer data and corroborate its binary nature in Pb-Hf-Nd isotope space. Along this segment, ϵ_{Hf} increases from a minimum value of +14 for subaerial RR peninsula samples to +18 for basalts dredged from 1000 meters below sea level. Meanwhile, Pb isotope ratios decrease from, respectively, 18.9, 15.5 and 38.3 to 18.3, 15.4 and 37.7 for $^{206}\text{Pb}/^{204}\text{Pb}$, $^{207}\text{Pb}/^{204}\text{Pb}$, and $^{208}\text{Pb}/^{204}\text{Pb}$. This steep Hf-Pb isotope gradient, which correlates with the steep topographic gradient, reflects the direct influence of the Iceland plume on RR MORB. Further south, down to 52.5°N (Gibbs FZ), as the topography descends more gently from 1000 to 2500 meters below sea level, basalts show nearly constant isotopic compositions at ϵ_{Hf} of +18 and $^{206}\text{Pb}/^{204}\text{Pb}$, $^{207}\text{Pb}/^{204}\text{Pb}$, and $^{208}\text{Pb}/^{204}\text{Pb}$ at 18.3, 15.4, and 37.6, respectively. Contrary to the 64-61°N segment, the homogeneous isotopic signal for the 61-52.5°N segment is decoupled from the topography. A spike in ϵ_{Hf} breaks the isotopic homogeneity at 57°N where two samples have values of +21. No similar spikes are observed for Pb or Nd isotopes, suggesting local Hf isotope decoupling, but a change occurs in the ridge axis bearing bending it to a more southerly direction. In the leaky Gibbs TZ, two samples have Pb isotope ratios slightly higher than neighbouring basalts, perhaps reflecting sediment incorporation during lava emplacement. Finally, from the Gibbs FZ to 50°N, the boundary where the influence of the Iceland and Azores plumes on the MAR meet, ϵ_{Hf} climbs steadily toward values exceeding +23, a tendency mirrored by gradually decreasing Pb isotope ratios. As opposed to the relatively more enriched basalts of the plateau, which may be under the influence of the Iceland plume, MORB in the vicinity of 50°N appear mostly unaffected by either the Iceland or the Azores plumes.

Short lifetime for CO₂ in the atmosphere after a meteorite impact on sediments

P. AGRINIER¹, A. DEUTSCH², U. SCHÄRER³ & I. MARTINEZ¹

¹IPG-Paris, 4 place Jussieu, F-75252 Paris France

²Univ. Münster, Münster, Germany

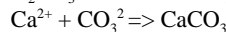
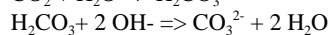
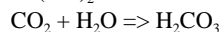
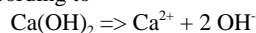
³Lab. Geochronologie, Univ. Nice, Nice, France

Impacts of large meteorite on Earth, such as Chicxulub impact at the K/T boundary, have been invoked to severely affect the surface of the Earth, leading to mass extinction. Of the most important are the greenhouse effects due to CO₂ released by decomposition of sedimentary carbonates (CaCO₃). In result, an equal amount of CaO is dispersed on the Earth surface.

We review chemical reactions that consume CaO and describe their consequences on the Earth ecosystem.

At temperature below 1000°C, CaO is very unstable in presence of CO₂ and is rapidly and quantitatively ($\approx 50\%$) transformed to CaCO₃ at 100 second timescale. The diffusion of CO₂ through CaCO₃ controls the kinetics.

At lower temperature ($\leq 100^\circ\text{C}$) CaO is not stable in contact of water and known to exothermically react to give portlandite : Ca(OH)₂. Then portlandite dissolves to buffer the water pH around 12.5 and in presence of CO₂, CaCO₃ forms according to



which is controlled by CO₂ diffusion in water and the dissolution rate of portlandite (S. Shih et al., 1999). Typical conversion rates are about 30 % of Ca(OH)₂ transformed into CaCO₃ within 20 minutes.

Such processes show that CO₂ lifetime in the atmosphere are controlled by the CaO reactivities at high and low temperatures. These lifetime may be very short.

References

- S. Shih et al., 1999, kinetics of the reaction of Ca(OH)₂ with CO₂ at low temperature; Ind. Eng. Chem. Res., 38, 1316-1322.

Thermodynamic description of aqueous non-electrolytes at infinite dilution over a wide range of state parameters

N. N. AKINFIEV^{1,2} AND L. W. DIAMOND²

¹Department of Chemistry, Moscow State Geological Prospecting Academy, Miklukho-Maklai str. 23, Moscow 117873, RUSSIA (akinfiev@unileoben.ac.at)

²Institut für Geowissenschaften, Abteilung Mineralogie und Petrologie, Peter Tunner Strasse 5, A-8700 Leoben, AUSTRIA (diamond@unileoben.ac.at)

An approach for describing the thermodynamic properties of aqueous non-electrolytes at infinite dilution is proposed. It is based on the accurate equation of state for the solvent (H₂O) given by Hill (1990) and requires only three empirical parameters that are independent of temperature and pressure. The master equation for chemical potential of the dissolved component μ_2 is:

$$\mu_2(P, T) = \mu_{2,g}(T) - RT \ln N_w + (1 - \xi) RT \ln f_1 + RT \xi \ln \left(\frac{R_v T}{M_1} \rho_1 \right) + RT \rho_1 \cdot \left(a + b \cdot \left(\frac{10^3}{T} \right)^{0.5} \right)$$

Here $\mu_{2,g}(T)$ stands for chemical potential of the pure gaseous component at temperature T and standard pressure $P = 1$ bar, $R = 1.987$ cal·mol⁻¹·K⁻¹ and $R_v = 83.14$ cm³·bar·K⁻¹·mol⁻¹ are gas constants, $N_w \approx 55.51$ mol/kg, M_1 , f_1 and ρ_1 denote molar mass (g/mol), fugacity (bar) and density (g/cm³) of the pure solvent (H₂O) at P - T conditions of interest, respectively, and ξ , a and b are empirical parameters that have definite physical meaning: ξ is introduced to describe the difference between intrinsic volumes of H₂O and the dissolved molecule (Plyasunov et al. 2000), and a and b characterise the difference in the short-range interaction energy between solute and solvent molecules. Thus, knowledge of the pure gas thermodynamic properties, together with these three parameters, enables prediction of the whole set thermodynamic properties of the solute at infinite dilution (chemical potential, entropy, molar volume, and apparent molar heat capacity) over a wide range of temperatures (0 - 500°C) and pressures (1 - 2000 bar), including the near-critical region. In the cases where experimental thermodynamic data are lacking, the empirical parameters could be estimated from the known standard-state properties of the solute only. The proposed approach has been tested for non-polar (Ar, Ne, H₂, N₂, O₂, CO₂) and polar (H₂S, NH₃, H₃BO₃, SiO_{2,aq}) dissolved molecules, ion pairs (HCl), and aqueous carbohydrates (CH₄, C₂H₄, C₂H₆, C₃H₈, C₄H₁₀, C₆H₆).

References

- Hill P.G. (1990), *J. Phys. Chem. Ref. Data*, **19**, 1233-1274.
 Plyasunov A.V., O'Connell J.P., Wood R.H. and Shock E.L. (2000) *Geochim. Cosmochim. Acta*, **64**, 2779-2795.

SHRIMP dating of lower crust xenoliths from Bering Sea region

V.V. AKININ¹, E. MILLER², J. WOODEN³

¹ North Eastern Interdisciplinary Science Research Institute, Russia (petrolog@neisri.magadan.ru)

² Stanford University, USA (miller@pangea.stanford.edu)

³ USGS, Menlo Park, USA (jwooden@usgs.gov)

The Late Cenozoic Bering Sea basalt province represents the most significant volume of alkali basalts erupted in the Arctic region within the last 10 Ma. Most of the volcanic fields are dominated by relatively LREE-enriched basalts with intraplate geochemical characteristics. Pb, Sr and Nd isotopic compositions of the basalts are diverse, indicating sources similar to those from MORB to OIB.

Trapped crustal xenolith suites in basalts include mostly undeformed, mafic Pl-Opx-Cpx cumulate rocks and pyroxene gneisses which equilibrated between 3 to 9 kb. Zircons were found in eleven plagioclase-bearing xenoliths from the Enmelen volcanoes (Chukchi Peninsula), and in one sample from the Imuruk volcanic field (Seward Peninsula) and were dated by the U-Pb method with the SHRIMP RG at Stanford University. Two types of zircons were observed - zoned prismatic ones (magmatic) and non-zoned rounded ones (metamorphic) with lower Th/U ratio. These data are combined with more limited results of a similar study of xenoliths from St. Lawrence Island basalts (Fig. 1).

Zircons from Enmelen mafic xenoliths indicate that 80-110 Ma magmatic rocks were involved in a younger thermal event between 60 and 75 Ma (peak at 70 Ma) that affected a large region of the deeper crust beneath the Bering Sea.

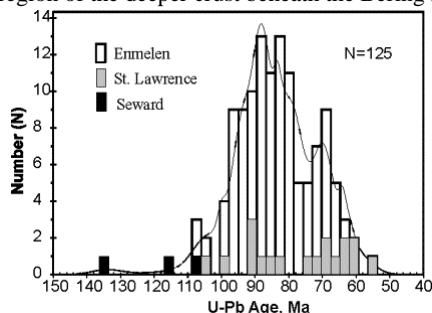


Figure 1. Histogram of U-Pb zircon ages from lower crust xenoliths of the Bering Sea basalt province.

The results suggest that the lower crust was significantly modified in the Cretaceous by magmatic underplating and heated again in the early Tertiary. These ages coincide with two major pulses of magmatism dated as 115-80 and 75-55 Ma which occurred together with and post-dated extensional collapse of previously thickened crust. Xenoliths ages thus reflect widespread signature of these events in the deep crust beneath the region.

This work funded partly by RFBR, grant 01-05-65453.

Mg-isotopes in terrestrial and extraterrestrial olivines.

O. ALARD¹, K.W. BURTON¹, P.A. BLAND² AND S.S. RUSSELL³

¹ Dept. Earth Science, The Open University, Milton Keynes MK7 6AA, U.K. (o.alard@open.ac.uk; k.w.burton@open.ac.uk).

² PSSRI, The Open University, Milton Keynes MK7 6AA, U.K. (p.a.bland@open.ac.uk).

³ Dept. Mineralogy, The Natural History Museum, London SW7 5BD, U.K. (sarr@nhm.ac.uk).

O-isotope studies of meteoritic materials have shown that the solar nebula was heterogeneous in composition, but also that some material as CAI and Ureilites have a non-mass dependant fractionation regime. Recent advances in MC-ICP-MS allow the investigation of other stable isotopic systems, and of particular interest are the 3-isotope systems of Fe and Mg (e.g. Zhu *et al.*, 2001; Galy *et al.*, 2000). Zhu *et al.* (2000) have shown that in a ⁵⁶Fe/⁵⁴Fe-⁵⁷Fe/⁵⁴Fe space terrestrial and extraterrestrial (chondrite and achondrite) materials plot on a single mass fractionation line, thus suggesting that the solar nebula was homogeneous in term of Fe-isotopes.

In this study Mg isotopes have been measured using MC-ICP-MS in terrestrial and extraterrestrial olivines, without chemical separation. Olivine has high Mg content, low minor/trace element contents, and is a rather ubiquitous phase. Analysis of Fe(Ni)-doped SRM-980 shows that there is no effect on the Mg isotopic composition. Furthermore, analysis of a number of mantle olivines (n=12; $\delta^{25}\text{Mg}=1.63\pm 0.06$; $\delta^{26}\text{Mg}=3.07\pm 0.08$, relative to SRM-980) shows a perfect agreement with the terrestrial mass fractionation line. Pallasite olivines have $\delta^{25}\text{Mg}$ ranging from 1.05 to 1.35 and show a mass dependant fractionation within error of the Terrestrial Fractionation Line (TFL). Ureilites show a wider range of Mg fractionation ($-0.30\leq\delta^{25}\text{Mg}\leq 1.54$), however, they still define a mass dependant fractionation line, with a slope indistinguishable to that of the TFL.

Mg isotopes depict a contrasting view of the solar nebula heterogeneity to that shown by O isotopes. No difference is observed between the pallasites (Vesta line in O- space) and the Earth. Ureilites show a mass dependant fractionation line in Mg isotopes which strongly contrasts with their slope (ca. 1) in O-space, yet is in agreement with the CAI Mg-isotopic composition (Galy *et al.*, 2000, Young *et al.*, 2002). These data suggest that the process/es responsible for O isotope fractionation did not affect Mg isotopes, or did not affect them in the same manner.

Galy A., Young E.D., Ash R.D., O'Nions R.K. (2000) *Science* **290**, 1751-1753.

Zhu X.K., Guo Y. O'Nions R.K., Young E.D., Ash R.D. (2001) *Nature* **412**, 311-313.

Young E.D., Ash R.D., Galy A., Belshaw N. (2002) *Geochim. Cosmochim Acta* **66**, 683-698.

A Lu/Hf and Sm/Nd perspective on the early differentiation of the Earth, Moon, Mars, and EPB

F.ALBAREDE¹, J.BLICHERT-TOFT¹, AND M.BOYET¹

¹ Ecole Normale Supérieure, 46 allée d'Italie, 69364 Lyon Cedex 7, France (albarede@ens-lyon.fr)

¹⁷⁶Lu-¹⁷⁶Hf and ¹⁴³Nd-¹⁴⁴Nd are the only two chronometric systems with long half-lives for which both the daughter and parent nuclides are refractory, lithophile, incompatible elements. The coupled Nd and Hf isotope systematics so far available for a large number of terrestrial and a few lunar samples [1,2] have now been extended to also include SNCs and eucrites [3,4]. Because the Earth, Mars, and the Moon all have post-formation histories, we consider the eucrite data together with data for these planets as chondrite-normalized source parent/daughter ratios.

On Earth, the coherence between Hf and Nd isotope ratios is strong with the mantle and the crust plotting in opposite quadrants of a (Lu/Hf)_N vs (Sm/Nd)_N plot. In most terrestrial basalts, Hf and Nd are more radiogenic than chondrites. Basaltic eucrites plot in the 'crustal' sector while cumulate eucrites plot in the 'mantle' sector. All lunar mare basalts plot in the 'mantle' sector: mildly radiogenic Hf and variable Nd for high-Ti basalts, and the opposite for low-Ti basalts. Finally, the most differentiated basaltic shergottites plot in the 'crustal' sector while the most cumulative shergottites fall in the mantle sector with relatively radiogenic Hf and variable Nd. The slope of the (Lu/Hf)_N vs (Sm/Nd)_N correlation increases in the order: Earth, Moon and Mars, eucrite parent body (EPB).

We believe that this relationship reflects the different thicknesses of the plagioclase stability field on the four planets. Terrestrial gravity is larger by factors of 3, 6, and, presumably, 40 with respect to Mars, the Moon, and the EPB, which gives a relative measure of the depth in the mantle that can produce plagioclase-saturated basalts. When compared with the Sm/Nd and Lu/Hf ratios of the major minerals that would crystallize from a chondritic magma ocean, we conclude that the mantle source of terrestrial basalts is controlled by equilibrium of melt with an olivine-clinopyroxene residuum. Plagioclase joins these two minerals in the source of SNCs and lunar mare basalts, notably the low-Ti basalts, and reaches a maximum in the mantle of the EPB. From Lu/Hf and Sm/Nd evidence only, it is unclear whether eucrites are small-degree melts from plagioclase-bearing cumulates or large-degree melts from a chondritic parent body. The low Ti contents and low Hf/Nd of cumulate eucrites and low-Ti lunar mare basalts indicate that either their parent magma or that of their mantle source lost substantial fractions of ilmenite. Cumulate eucrites therefore represent gabbros soaked by extremely differentiated melts.

References

- [1] Unruh D.M. et al. (1984) *JGR* **89**, B459-B477 [2] Beard B.L. et al. (1998) *GCA* **62**, 525-544 [3] Blichert-Toft J. et al. (1999) *EPSL* **173**, 25-39 [4] *id* (2002) this meeting.

Zoned mantle convection

F. ALBAREDE¹ AND R. D. VAN DER HILST²

¹ Ecole Normale Supérieure, 46 allée d'Italie, 69364 Lyon
Cedex 7, France (albarede@ens-lyon.fr)

² MIT, Cambridge, MA 02139, USA

We review the present state of understanding of mantle convection with respect to geochemical and geophysical evidence, and we suggest a model for mantle convection and its evolution over Earth's history that can reconcile this evidence. Whole mantle convection, even with material segregated within the D" region just above the core mantle boundary, is incompatible with the budget of argon and helium and with the inventory of heat sources required by the thermal evolution of the Earth. We show that the deep mantle composition in lithophile incompatible elements is inconsistent with the storage of old plates of ordinary oceanic lithosphere, i.e., with the concept of plate graveyard. Isotopic inventories indicate that the deep mantle composition is not correctly accounted for by continental debris, primitive material, or subducted slabs containing normal oceanic crust. Seismological observations have begun to hint at compositional heterogeneity in the bottom 1000 km or so of the mantle, but there is no compelling evidence in support of an interface between deep and shallow mantle at mid-depth.

We suggest that in a system of thermo-chemical convection lithospheric plates subduct to a depth that depends on their composition and thermal structure. The thermal structure of the sinking plates is primarily determined by the direction and rate of convergence, the age of the lithosphere at the trench, the sinking rate, and the variation of these parameters over time (i.e., plate tectonic history) and is not the same for all subduction systems. The sinking rate in the mantle is determined by a combination of thermal (negative) and compositional buoyancy, and as regards the latter we consider in particular the effect of the loading of plates with basaltic plateaus produced by plume heads. Barren oceanic plates are relatively buoyant and may preferentially be recycled in the shallow mantle. Oceanic plateau-laden plates have more pronounced negative buoyancy and can more easily founder to the very base of the mantle. Plateau segregation remains statistical and no sharp compositional interface is expected from the multiple fate of the plates.

We show that the variable depth subduction of heavily laden plates can prevent full vertical mixing and preserve a vertical concentration gradient in the mantle. In addition, it can account for the preservation of scattered remnants of primitive material in the deep mantle and therefore for the Ar and ³He observations in ocean island basalts.

Oxygen isotopic composition of single aerosol particles: a study of Saharan dust sources

J. ALÉON¹, M. CHAUSSIDON², B. MARTY², L. SCHÜTZ³
AND R. JAENICKE³

¹ UCLA, Dept Earth Space Sciences, Los Angeles, USA,
(aleon@ess.ucla.edu)

² CRPG-CNRS, Vandoeuvre-les-Nancy, France.

³ Institut für Phys. der Atmosph., J. Gutenberg Univ., Mainz,
Germany.

To understand the climatic impact of mineral dust in the atmosphere, emission mechanisms and source strength must be known in addition to the dust physico-chemical properties. A new method to estimate the sources of mineral dust independently from atmospheric observation is reported here. The O isotopic composition of individual quartz grains from 2 to 10 µm were measured in an aerosol sample collected over the Cape Verde islands and in 4 soils from Saharan regions having strong dust emission rates (Morocco, Algeria, Niger and Chad). O isotopes were also measured in coarse-grained quartz from the soils to study their relationship with geological sources.

O isotope ratios were measured by ion microprobe microbeam (1 µm) analysis, after chemical isolation of quartz (Syers et al., 1968). Grains of interest were located by imaging of ¹⁶O and then measured individually using an electron multiplier. The internal precision and external reproducibility were close to 3‰. Coarse grains were measured using multicollection and Faraday cup detectors with a precision close to 0.5‰.

$\delta^{18}\text{O}$ values of quartz in the coarse soil fractions can be compared with the major geological formation of each region indicating that each soil can be considered representative of regions ~100×100 km. More distal contributions in the 2-10 µm fractions suggest a regional aeolian mixing by low intensity winds. Differences between the fine fractions from soil to soil indicates that this mixing does not exist at the 1000 km scale. $\delta^{18}\text{O}$ values of aerosol quartz are comparable with the soil fine fractions. The highest $\delta^{18}\text{O}$ values (+30 to +40‰) observed in the aerosol and in some soil fine fractions are attributed to lacustrine cherts formed in evaporitic environments in the Chad basin. Their proportions and the direct comparison of the $\delta^{18}\text{O}$ distributions indicate that the most probable source of the sampled dust event is the Niger region. These observations suggest that dust in the Sahara is regionally mixed by low intensity winds but not globally and that dust carried over long distances is emitted in the high troposphere by temporally and spatially discrete dust storms.

References

Syers J. K., Chapman S. L., Jackson M. L., Rex R. W and Clayton R. N. (1968) *Geochim. Cosmochim. Acta* **32**, 1022-1025.

How did chondrules/CAIs acquire their O anomalies?

C.M.O'D. ALEXANDER

Dept. Terrestrial Magnetism, Carnegie Institution of Washington, 5241 Broad Branch Rd. NW, Washington, DC 20015, USA (alexande@dtm.ciw.edu)

The O isotopes of type B CAIs and chondrules, except in enstatite chondrites, lie on mixing lines with slopes of ~ 1 . These O isotopic compositions were likely established by gas-melt exchange. The initial isotopic compositions of the gas and the dust/melt remain unresolved. The Earth-Moon, Mars, CI- and E-chondrites, fall on very similar mass fractionation lines, consistent with the bulk composition of the nebula being close to terrestrial values. The pattern of O isotopic compositions in CC-chondrite chondrules and CAIs points to dust/melt ($\delta^{17,18}\text{O} \approx -50\%$) exchanging with a gas composition lying near $\delta^{17,18}\text{O} \approx 0\%$ (e.g. Clayton, 1993). The lack of mass independent fractionation in EC chondrules hints at a fractionation mechanism that is redox sensitive.

The main O-bearing species in the nebular gas were H_2O and CO. Modelling indicates that under relatively oxidizing conditions H_2O would have interacted with a melt more rapidly than CO, via evaporation/condensation [e.g. $\text{SiO}(\text{g}) + \text{H}_2\text{O}(\text{g}) = \text{SiO}_2(\text{l}) + \text{H}_2$] and gas-melt exchange. Also, CO- H_2O isotopic exchange would have been rapid compared to gas-melt exchange.

If the initial dust/melt composition was $\delta^{17,18}\text{O} \approx -50\%$, the initial gas composition must have been above the terrestrial mass fractionation line. It requires that gas-dust equilibration in the Earth-Moon, Mars, CI-, and E-chondrite formation regions involved remarkably similar dust/gas ratios despite their very different locations and bulk chemistries. It also leaves the lack of mass independent fractionation in EC chondrules unexplained.

Alternatively, the gas and dust both had compositions near $\delta^{17,18}\text{O} \approx 0\%$, and the mass independent fractionation occurred in the gas during chondrule/CAI formation. To explain the generally lighter O isotopic compositions of the more refractory chondrules/CAIs, isotopically light H_2O ($\delta^{17,18}\text{O} < -50\%$) must be generated near peak temperatures, but H_2O become heavier with time/cooling. Of the 4 reactions not involving ozone known to produce mass independent fractionation (Thiemens, 1999), only $\text{OH} + \text{CO} = \text{CO}_2 + \text{H}$ has been modelled to date. This reaction preferentially consumes C^{16}O . To produce $\delta^{17,18}\text{O} \approx -50\%$ H_2O , requires that C^{16}O react $\sim 25\%$ faster than the other isotopomers. The reaction would become less important under reducing conditions as the OH and H_2O would be converted to CO. However, the overall reaction rate does not exhibit the required temperature sensitivity. It remains to be seen whether any of the other reactions have the appropriate properties to make this a viable explanation.

References

Clayton R.N., (1993), *Ann. Rev. E. Planet. Sci.* **21**, 115-149.
Thiemens M.H., (1999), *Science* **283**, 341-345.

Study of diatoms/aqueous solution interface: I. Testing a surface complexation approach

ALEXANDRE, G.¹, POKROVSKY O.S.¹, SCHOTT J.¹, BOUDOU A.², FEURTET-MAZEL A.², MIELCZARSKI E.³, MIELCZARSKI J.³, SPALLA O.⁴

¹Géochimie transferts et mécanismes, CNRS-OMP-Université Paul Sabatier, 38 rue des 36 Ponts, 31400 Toulouse, France

²LEESA, UMR CNRS 5805, Université Bordeaux 1, Place du Dr Peyneau, 33120 Arcachon, France

³LEM, UA 235 CNRS, INPL-ENSG, B.P. 40 Vandœuvre-lès-Nancy 54501 France

⁴CEA/DSM, Service de Chimie Moléculaire, 91191 Gif sur Yvette Cedex, France

This work reports on a concerted study of diatom trace metals-water interfaces with four different species: two marine planktonic species (*Thalassiosira weissflogii*, *Skeletonema costatum*) and two freshwater periphytic species (*Achnantes minutissima*, *Navicula minima*). Cell surface charge was measured by potentiometric titration using a limited residence time reactor. The zeta potential of living cells was determined in a wide range of solution composition (pH, ionic strength, dissolved organic matter and metals concentrations). Information on the chemical composition and molecular structure of diatoms surfaces was obtained using FT-IR (Diffuse Reflectance and Attenuated Total Reflectance) and X-ray Photoelectron Spectroscopy (XPS). The surface area of living cells in aqueous solutions was quantified using Small Angle X-ray Scattering Spectroscopy (SAXS).

These observations allowed the identification of the major specific surface functional groups. Taking into account the high specific surface area of viable cells as measured by SAXS (on the order of $10^{-7} \text{ m}^2/\text{cell}$) and relative proportion of carboxylic, amine and silanol surface sites of 1:1:0.02 as inferred from XPS and FT-IR quantification of *Achnantes Minutissima* cells wall composition, a surface complexation model (SCM) was constructed that allows a rigorous thermodynamic description of diatom-solution interfaces. A good agreement between the experimental data and surface complexation modeling demonstrates the validity of this thermodynamic approach.

Preliminary experiments on metal adsorption (Cd, Pb, U, and Al) on two marine and two freshwater diatom species evidenced very fast and reversible processes which can be modeled within the framework of SCMs recently developed for complex multioxide minerals and carbonates (Pokrovsky & Schott, 2002) and bacterial surfaces (Fein et al., 1997).

New developments in measuring silicon isotopes by MC-ICP-MS

L. ALLEMAN¹, D. CARDINAL¹, K. ZIEGLER² AND L. ANDRÉ¹

¹Royal Museum for Central Africa - Dept. of Geology - Leuvensesteenweg, 13 - B3080 Tervuren - Belgium (lalleman@africamuseum.be; dcardinal@africamuseum.be; lucandre@africamuseum.be)

²Dept. of Geography Research, Ellison Hall 3611 University of California, Santa Barbara, CA 93106, U.S.A. (kziegler@geog.ucsb.edu)

Introduction

A MC-ICP-MS (Multi Collector Inductively Plasma Mass Spectrometer from Nu Instruments) has been tested to precisely detect variations in the isotopic composition of Si on several samples.

Results and Discussion

Variation in sample $^{28}\text{Si}/^{29}\text{Si}$ ratios are expressed as $\delta^{29}\text{Si}$ units, which represent deviations in ‰ from the same ratio in a sample relative to a quartz standard measured using the bracketing "standard-sample-standard" technique. Taking into account the interferences of N_2 , CO and NO in the Si mass region, and measuring in dynamic mode the Mg isotopes as internal standard, the repeatability on the $\delta^{29}\text{Si}$ measurements is better than 0.15 ‰ and its individual precision better than 0.05 ‰. Its accuracy is estimated by inter-laboratory comparison. Factors that are found to strongly affect the precision and accuracy of isotope ratio measurements by MC-ICP-MS are mass discrimination of interferences, drift of the isotope ratio and matrix effects. We will present the results obtained on natural silica and opal (quartz, diatoms, sponges) and artificial samples. We will discuss the various analytical methodologies tested (e.g., dry/wet plasma, sample dissolution, Si/Mg ratios, sensitivity).

Conclusion

These results are of great relevance regarding environmental and geological sciences where Si isotopes could open up a range of new analytical studies. Moreover, the MC-ICP-MS technique has obvious advantages over previous mass spectrometry techniques used to determine Si isotope ratios. The sample introduction system does not request handling dangerous chemicals and the instrument presents very good precision and sensitivity.

The relationship between the marine and the terrestrial (speleothems) climatic record during the last 80 ka in the Eastern Mediterranean

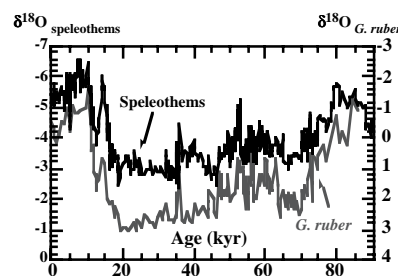
A. ALMOGI-LABIN¹, M. BAR-MATTHEWS¹, M. PATERNE², A. AYALON¹, B. SCHILMAN¹

¹Geological Survey of Israel, 30 Malchei Israel St. Jerusalem, 95501, Israel (almogi@mail.gsi.gov.il; matthews@mail.gsi.gov.il; ayalon@mail.gsi.gov.il; bettina.shilman@mail.gsi.gov.il)

²LSCE -CNRS-CEA Avenue de la Terrasse 91198 Gif sur Yvette, France (Martine.Paterne@lsce.cnrs-gif.fr)

Among the key questions in paleoclimate studies is the extent of the connection between the marine and the land records. This covers issues of heat transfer, rainfall generation, and timing of climatic events. The present study explores this connection by comparing high resolution $\delta^{18}\text{O}$ records covering the last 80 kyr of planktonic foraminifera *G. ruber* from a core located off the Israeli coast, with the well-dated (U-Th) high resolution record of speleothems from the Soreq cave, located ~40 km inland.

There is a striking similarity between the two profiles (Fig. 1). The most pronounced features of the last glacial are the high amplitude $\delta^{18}\text{O}$ fluctuations during marine isotope stage 3, compared with the relatively constant and higher $\delta^{18}\text{O}$ values during marine isotope stages 4 and 2. Highest sedimentation rate and speleothem growth occurred between 34 and 36 kyr and from 52 to 57 kyr and are associated with the lowest $\delta^{18}\text{O}$ values.



Under present-day conditions the $\Delta\delta^{18}\text{O}_{G.ruber-speleothems}$ is 5.5‰ due to the fractionation between the sea surface $\delta^{18}\text{O}$ and the rainfall on-land. During interglacial sapropel events the $\Delta\delta^{18}\text{O}_{G.ruber-speleothems}$ are the lowest ~4‰, and immediately after the values increase towards present-day values. During glacial intervals when speleothems and *G. ruber* $\delta^{18}\text{O}$ have the highest values, the $\Delta\delta^{18}\text{O}_{G.ruber-speleothems}$ is the largest reaching 6.5‰. Between 60 and 45 kyr the $\Delta\delta^{18}\text{O}_{G.ruber-speleothems}$ fluctuate largely due to climate instability as reflected by the large $\delta^{18}\text{O}$ fluctuations of *G. ruber* and the speleothems. Thus, the changes in $\Delta\delta^{18}\text{O}_{G.ruber-speleothems}$ reflect the humidity differences between sea and land.

Size effects on colloids diffusion in granite micro fractures

U. ALONSO¹, T. MISSANA¹, A. PATELLI²,
V. RIGATO², J. RAVAGNAN²

¹ CIEMAT, Avda. Complutense 22- Edif. 19, 28040 Madrid
SPAIN (e-mail: ursula.alonso@ciemat.es)

² INFN-LNL, Via Romea 4, 35020 Legnaro-Padova ITALY

Clay colloids can be generated at the host rock (granite)/engineered barrier (bentonite) interface of a deep geological radioactive waste repository (1). The migration of these clay particles into the rock micro-fractures could affect the migration rate of those radionuclides presenting significant sorption onto the clay.

In previous experiments simulating the bentonite/granite interface of a repository, the migration of clay particles through granite micro-fractures was observed. Furthermore, the transport of contaminants (U, Cs and Eu) sorbed onto bentonite particles was also detected (2). The study of the granite micro-fracture network structure by laser confocal microscopy revealed that particles with size lower than few μm might have entered and migrated through the rock. It is therefore very important to understand the diffusion behaviour of colloids within the rock matrix, taking into account a crucial parameter as the size.

In this work, nuclear ion beam techniques such as RBS (Rutherford Backscattering) and micro-PIXE (Microbeam-Particle Induced X-Ray emission) were used for studying the extent of colloid diffusion through granite micro-fractures as a function of the colloid size.

Gold colloids were selected as diffusants because of their suitability in natural environments; in fact, they are easily identified in geological materials (both in clay and granite), they are available in different and mono-disperse size distributions and they are stables in natural waters conditions. For these studies, granite slices were put in contact with two different gold colloid suspensions (with diameters of 40 nm and 100 nm respectively) allowing the diffusion of the particles within the rock. After the contact, the samples were analyzed by means of RBS and micro-PIXE. In all cases, a gold diffusion profile was detected inside the granite showing a clear dependence on the particle size; the lower the particle diameter, the faster diffusion process.

The fact that the diffusion of particles through granite is observed states the importance of studying colloid mediated transport of contaminants in porous rocks.

This work was partially supported by the EU within the 4th and 5th Framework Programs TMR-LSF, contract numbers ERBFMGECT980110, HPRI-1999-CT-00083.

(1) Missana T., Alonso U., Turrero M.J., J. Cont. Hydr. (2002), Accepted

(2) Alonso, U., Missana, T., Patelli, A., Rigato, V., Rivas, P., J. of Cont. Hydrol. (2002) Accepted.

Some textural and geochemical evidences on mixing and mingling in the genesis of Karamagara Volcanics, Saraykent-Yozgat, Central Anatolia, Turkey

MUSA ALPASLAN¹, NAZMI OTLU², TANER EKICI²,
ABIDIN TEMEL³, DURMUS BOZTUG²

¹Mersin University, Department of Geology, 33343,
Mersin/TURKEY, malpaslan@mersin.edu.tr

²Cumhuriyet University, Department of Geology, 58140-
Sivas/Turkey, notlu@cumhuriyet.edu.tr,
ekici@cumhuriyet.edu.tr, boztug@cumhuriyet.edu.tr

³Hacettepe University, Department of Geology, Beytepe-
Ankara/Turkey, atemel@hacettepe.edu.tr

Plio-Quaternary Karamagara andesitic lava flows are exposed in Saraykent (Yozgat) region. These volcanics have a hypocrystalline-porphyritic texture and include the clinopyroxene, hornblende and plagioclase phenocrysts. Olivine and hornblende xenocrysts have also been seen in these volcanics. Subrounded to rounded magmatic enclaves, ranging from a few mm to decimeter in size, are present in Karamagara volcanics. The enclaves are range from basaltic andesite to andesite in composition, and generally have a vitrophyric-propyritic texture but some enclaves have the holocrystalline texture. Some distinctive mineral textures have been seen such as sieve-textured plagioclases, hornblendes with an appinitic texture and a reaction rim exhibit the disequilibrium crystallization with host magma. Enclaves and olivine xenocrysts also show the mingling process in the evolution of the volcanics.

Geochemistry of the Karamagara volcanics and enclaves reveal the magma mixing process in the evolution of these volcanics. K/Sr-Ba/Rb diagram exhibits that they are fitted on the mixing line. On the other hand, holocrystalline enclaves and hornblende xenocrysts surrounded by clinopyroxene microlithes suggest that stratification in the magma chamber were broken down, and crustal assimilation, respectively. Insights of above data, it can be suggested that the Karama_ara volcanics have the complex evolution history such as mixing, mingling and crustal assimilation processes.

Nd concentration and isotopic ratio in the waters of the Pacific Ocean

HIROSHI AMAKAWA¹, DIA SOTTO ALIBO², KIYOTAKA FUKUGAWA², JING ZHANG³ AND YOSHIYUKI NOZAKI²

¹Tokyo Metropolitan University, Hachioji, Tokyo, Japan (amakawa@comp.metro-u.ac.jp)

²Ocean Research Institute, University of Tokyo, Nakano, Tokyo, Japan

³Toyama University, Toyama, Japan

Four vertical profiles of dissolved Nd concentration and isotopic ratio were determined in the northwest Pacific near the Japanese Islands.

As for the stations in the Kuroshio Current regime (LM2, LM6/11), depth profiles of Nd isotopic ratio is not so smooth. The depth profiles at LM2 (29°N, 143°E) and LM6/11 (34°N, 142°E) have two minima at ~250m ($\epsilon_{Nd} = -7.4$ for LM2, -8.7 for LM6/11) and ~2000m ($\epsilon_{Nd} = -6 \sim -5$) and one maximum around 800 ~ 1000m. The stations in the Oyashio Current regime (LM9, CM5) show less complicated Nd isotopic vertical profiles compared with those in the Kuroshio. Within the depth range of 800 ~ 1000m, LM9 (40°N, 145°E) and CM5 (40°N, 155°E) show almost same values as those at LM2 and LM6/11, which seems to be due to the influence of the North Pacific Intermediate Water (NPIW) to both the Kuroshio and Oyashio Current regimes. Except for the surface, the profile of CM5 is almost as same as that of the previously reported subarctic site, TPS 47 39-1 (Piepgras and Jacobsen (1988)). On the other hand, below 1000m, LM9, located in the southern edge of the Oyashio Current regime, shows less radiogenic values compared with CM5 and TPS 47 39-1.

The shallow Nd isotopic minimum observed in the Kuroshio Current region is due to the contribution of the North Pacific Tropical Water (NPTW), which might be supplied large amount of the continental derived Nd from the South China Sea or East China Sea. As the samples from the depths around NPTW do not show any characteristic REE patterns, the Nd isotopic ratios are the only indicators for the water mass.

Within the depth range of 1000 to 5000m, the Nd isotopic profile at CM5 shows the slight but clear radiogenic ratios compared with LM stations. This strongly suggests the limited deep water exchange between CM5 and those at LM stations. The vertical processes might play a key role in the formation of the water mass with high Nd isotopic ratio in the subarctic area.

Overall, the combined Nd isotopic and Nd concentration (REE pattern) study gives the various information on the water circulation and vertical processes in the ocean.

References

Piepgras DJ and Jacobsen SB (1988) *Geochim. Cosmochim. Acta* **56**, 1851-1862.

Pb isotopic dating of chondrules

Y. AMELIN¹, E. ROTENBERG¹ AND A. N. KROT²

¹ Department of Earth Sciences, Royal Ontario Museum, Toronto, ON M5S 2C6, Canada (yuria@rom.on.ca, ethanr@rom.on.ca)

² Hawaii Institute of Geophysics and Planetology, University of Hawaii at Manoa, Honolulu, HI 96822, USA (sasha@higp.hawaii.edu)

Introduction

Chondritic meteorites consist of three major components: Ca, Al-rich inclusions (CAIs), ferromagnesian silicate chondrules, and fine-grained matrix. The timing of chondrule formation and time interval between the formation of CAIs and chondrules could provide important constraints on their origin and solar nebula evolution, but remain unknown.

Short-lived isotope chronometers ²⁶Al-²⁶Mg, ⁵³Mn-⁵³Cr and ¹²⁹I-¹²⁹Xe allow precise dating of chondrules, but depend on assumptions about the distribution and initial abundances of parent radioactive isotopes, and give relative ages only. Radiogenic ²⁰⁷Pb/²⁰⁶Pb ratios provide absolute ages with a similar precision of $\pm 1-2$ m.y. or better. The precision and accuracy depend on effective removal of common Pb, and on establishing high quality Pb-Pb isochron relationships. With modern low-blank (1-2 pg) techniques for Pb isotope analyses it is possible to obtain precise and highly radiogenic Pb isotopic ratios from 1-10 mg of chondrule silicates, large single chondrules, or groups of several smaller chondrules.

Results

Pb isotope data for the CR2 chondrite Acfer 059 illustrate the potential and problems of chondrule dating. Twenty seven silicate fractions from this meteorite yielded ²⁰⁶Pb/²⁰⁴Pb ratios between 11.09 (matrix) and 2200 (one of acid-washed chondrules). Pb-Pb "errorchron" regression of all data yields 4562.8 ± 3.4 Ma with MSWD=52. Data for all 23 acid-washed and unwashed chondrules with ²⁰⁶Pb/²⁰⁴Pb ≥ 17.8 yield an "errorchron" date of 4563.3 ± 1.9 Ma (MSWD=19). The six most radiogenic Pb isotope data points from acid-washed chondrules with ²⁰⁶Pb/²⁰⁴Pb ≥ 395 define an isochron with an age of 4564.7 ± 0.6 Ma, MSWD=0.5 (Amelin and Krot 2002). Increasing scatter for less radiogenic data suggests that the common Pb isotopic heterogeneity is the main threat to precision of Pb isotope dating.

The efficiency of acid washing for minimising common Pb content varies between meteorites, and the precision of chondrule dates varies accordingly. Nine chondrules with ²⁰⁶Pb/²⁰⁴Pb ratios between 50-171 from the CV3 chondrite Allende yielded an isochron with an age of 4566.8 ± 1.6 Ma (MSWD=1.3). Tentative less radiogenic data from the CR2 chondrite Renazzo and LL3.1 chondrite Krymka define less precise "errorchrons" giving the dates of 4564 ± 12 Ma, MSWD=11.5, and 4576 ± 18 Ma, MSWD=10.7.

References

Amelin Y. and Krot A. N. (2002) Submitted to the Annual Meeting of the Meteoritical Society.

The crystallisation of colloidal As-S phases: an *in situ* X-ray diffraction study

AMOR KENNETH, BENNING LIANE.G*.

School of Earth Sciences, University of Leeds, Leeds, UK

(*corresponding author: liane@earth.leeds.ac.uk)

The precipitation of sparingly soluble As^{III} sulphides occurs in many natural environments and their formation controls a large part of the global arsenic cycle. However, the formation mechanisms of arsenic sulphide minerals are poorly understood due to the lack of thermodynamic and kinetic data pertaining to their nucleation and growth. The main crystalline As-S phases in aqueous solutions below 300°C are orpiment, As₂S₃, and realgar, AsS and these phases form under very specific chemical and physical conditions (pH, redox, temperature) and are therefore, very accurate geochemical indicators. Below 100°C a mixture of aqueous As^{III} and H₂S instantly precipitates a poorly ordered colloidal As-S suspension (of As₂S₃ composition) but the transformation of this colloid into crystalline orpiment or realgar requires either a structural ordering or a change in sulphur and arsenic oxidation states. The crystallisation of the amorphous precursor occurs in nature below 100°C, yet this process has only been achieved in the lab at high temperatures from the melt. The kinetics and activation energies for this process at hydrothermal temperatures and in aqueous solutions are not known.

In this study, the chemical and physical conditions controlling the nucleation and growth of crystalline orpiment from the amorphous colloidal As₂S₃ precursor were evaluated experimentally using *in situ* synchrotron-based energy dispersive X-ray diffraction (ED-XDR). The experiments were carried out *in situ*, in reducing hydrosulphide solutions and at temperatures between 75 and 260°C. The time dependent changes in Bragg peak areas and intensities were used to derive information about the nucleation and growth kinetics of crystalline orpiment. In addition, the real time data were used to determine the reaction mechanisms and the activation energy for the formation of orpiment from reduced, aqueous sulphide solutions at hydrothermal conditions.

Dissolution kinetics of smectite under acidic conditions

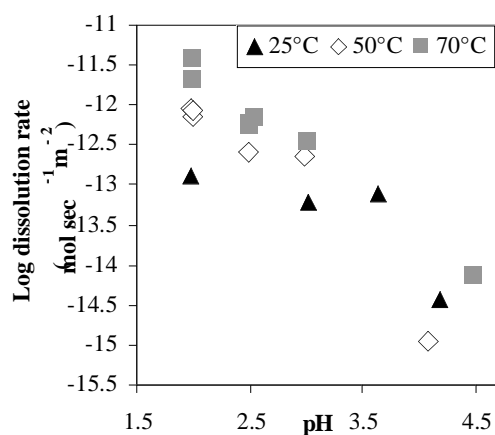
K. AMRAM AND J. GANOR.

Dept. Geol. & Env. Sci., Ben-Gurion Univ. of the Negev,
Beer-Sheva 84105, Israel (kamram@bgumail.bgu.ac.il)
(ganor@bgumail.bgu.ac.il)

Smectite was selected as a potential sealant in the multibarrier systems designated for storage of radioactive waste. A major concern, which directly affects the protective properties of the barrier, is the dissolution and precipitation of smectite. Interpretation and modelling of the environmental processes strongly depend on our understanding of the environmental parameters that control the rate of dissolution and precipitation. For this reason, flow-through experiments were carried out to study the effect of pH and temperature on the dissolution rate of smectite.

Smectite dissolution rate (Fig.1) varies as a function of temperature and fluid composition from $1.88 \cdot 10^{-15} \text{ mol m}^{-2} \text{ s}^{-1}$ (at 50°C and pH 4) to $3.64 \cdot 10^{-12} \text{ mol m}^{-2} \text{ s}^{-1}$ (at 70°C and pH 2). Dissolution rate increases with temperature and decreases with increasing pH. Apparent activation energies were calculated from the slope of log rate vs. the temperature reciprocal. As the pH decreases the apparent activation energy increases from 8 kcal/mol at pH 3 to 14 kcal/mol at pH 2. Although the observations may be described reasonably well by a single proton promoted mechanism as is evident by the steady increase in rate with decreasing pH (Fig. 1), detailed examination of the data shows that between pH 3 and 2.5 the dissolution rate remains relatively constant. The change in slope and the pH dependence of the apparent activation energy may indicate that more than one reaction mechanism controls the rate, as was suggested for kaolinite dissolution by Cama et al. (2002).

Fig. 1: The effect of pH and on smectite dissolution rate



Reference:

Cama J., Metz V., and Ganor J. (2002), *Geochim. Cosmochim. Acta*, submitted.

Geochemistry of the Salton Sea, CA

C. AMRHEIN, I. R. RODRIGUEZ, AND J. P. DE KOFF

University of California, Riverside, Dept. of Environmental Sciences. (amrhein@ucr.edu)

The Salton Sea is a saline, closed basin lake 70 meters below MSL in the southern desert of California. The sea has a surface area of 945 km², a volume of 9.25 km³, a mean depth of 9 m, and an annual inflow of 1,600 million m³. The sea formed in 1905, and is sustained by excess irrigation water from the Colorado River and municipal wastewater. It is hyper-eutrophic due to fertilizer inputs from farm runoff, and has recently been identified as containing the highest density of fish of any body of water of this size. The salinity is currently 43,000-mg/kg, containing 10,200-mg/kg sulfate and 16,800-mg/kg chloride. The salinity of the sea is rising and there are concerns that within a few decades the fish will be gone. Plans are being considered for construction of a salt repository to control salinization and maintain the sea as a refuge for migratory waterfowl. Additionally, there is interest in reducing the phosphate loading to reduce algae blooms and improve water quality. Sulfate reduction is a major process of organic matter oxidation within the sediments and extensive outgassing of hydrogen sulfide occurs during wind events. Periods of anoxia throughout the water column can occur during the hot summer months and massive fish kills are common. Calcite, gypsum, pyrite, and green rust (II) are precipitating and accumulating in the sediments. We conducted an extensive sampling of the sediments and measured the amounts of these minerals. We have estimated the annual rate of mineral formation based on mass balance calculations and geochemical calculations. This information is needed to determine the rate salinity increase and the timetable for construction of a salt repository. Laboratory experiments indicate that coprecipitation of phosphate with calcite is an important mechanism reducing the internal loading of P and limiting algae blooms. Thus, source control of P from farmers' fields will lead to significant reductions in algae blooms and a reduction in hydrogen sulfide production.

Iron isotopes in an Archean paleosol

A. D. ANBAR¹, G. L. ARNOLD¹, R. RYE², S. WEYER³

¹Department of Earth and Environmental Sciences, University of Rochester, Rochester, NY 14627 USA
(anbar@earth.rochester.edu; gail@earth.rochester.edu)

²Department of Earth Sciences, University of Southern California, Los Angeles, CA 90089 (rye@usc.edu) USA

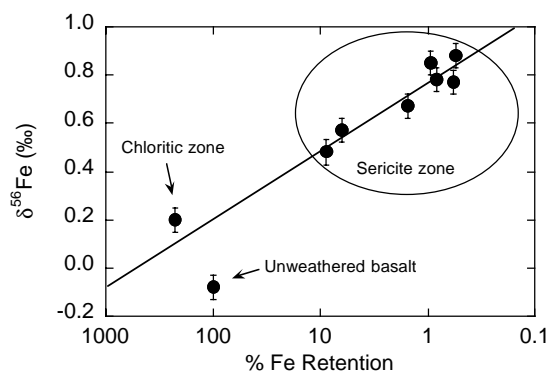
³ThermoFinnigan MAT, Bremen, Germany
(sweyer@ThermoFinniganMAT.de)

Motivation and Methods

The Fe-depleted Mt. Roe #2 (W. Australia) paleosol was formed ~ 2.75 Ga. Low pO₂ in the Archean atmosphere probably facilitated Fe loss. We have analysed the Fe isotope composition of this paleosol to gain insight into the mechanisms of Fe mobilization.

Iron isotope compositions were determined by high-resolution multiple-collector ICP-MS (Neptune, ThermoFinnigan MAT, Bremen, Germany). Prior to analysis, Fe was extracted from samples using anion exchange chromatography. Instrument mass bias was corrected with a Cu "element spike". Using a high-resolution entrance slit and low-resolution collector slits, isobaric interferences from ArO⁺, ArN⁺ and ArOH⁺ were resolved sufficiently to observe a mass-dependent relationship between $\delta^{56}\text{Fe}$ and $\delta^{57}\text{Fe}$. External precision (1 σ) on $\delta^{56}\text{Fe}$ and $\delta^{57}\text{Fe}$ was better than ± 0.05 and 0.08 ‰, respectively.

Figure 1: $\delta^{56}\text{Fe}$ vs. % Fe retention



Results are shown in Fig. 1. $\delta^{56}\text{Fe}$ is reported relative to the IRMM standard. Fe retention is calculated relative to the underlying basalt on a Ti-normalized basis.

$\delta^{56}\text{Fe}$ of the basalt parent material is ~ -0.1 ‰; all other samples are enriched in ⁵⁶Fe. Fe isotope fractionation confirms that low Fe concentrations in the sericite zone result from Fe loss, and reveals preferential loss of light Fe isotopes. $\delta^{56}\text{Fe}$ in the sericite zone fits a Rayleigh trend ($\alpha \sim 1.00012$) with initial $\delta^{56}\text{Fe}$ similar to chloritic Fe. The data are consistent with Fe loss during chlorite formation and a kinetic isotope effect during weathering (Brantley et al., 2001), although other mechanisms are possible.

Reference

Brantley, S.L., Liermann, L. and Bullen, T.D. (2001), *Geology* **29**, 535-538.

Influence of inclusions and leaching techniques on Sm-Nd and Lu-Hf garnet chronology

ROBERT ANCZKIEWICZ^{1,2} MATTHEW THIRLWALL² AND JOHN PLATT¹

¹University College London, Gower Street, London WC1E 6BT, UK (rob@gl.rhul.ac.uk)

²Royal Holloway University of London, Egham, Surrey TW20 OEX, UK (m.thirlwall@gl.rhul.ac.uk)

Sm-Nd chronology is often affected by REE-rich inclusions, which lead to ambiguous ages, lower precision or make dating impossible. In order to investigate this problem we conducted Lu-Hf and Sm-Nd garnet dating on a high pressure granulite, a felsic subvolcanic intrusion and a high grade metapelite. We propose a new leaching technique capable of substantially reducing or even eliminating phosphate inclusions.

Lu-Hf and Sm-Nd dating of high pressure garnet granulite from Kohistan region of Pakistan yielded concordant ages of 94 ± 1.2 and 95.9 ± 2.6 Ma respectively. Small variations in both $^{176}\text{Lu}/^{177}\text{Hf}$ and $^{147}\text{Sm}/^{144}\text{Nd}$ ratios among 3 garnet fractions result most likely from small amount of amphibole contamination. Dating of the subvolcanic intrusion from Lanarkshire (Scotland) gave a Lu-Hf age of 419 ± 19 Ma, concordant with the 411 ± 2 Ma Sm-Nd age of Thirlwall (1988). Poor precision of Lu-Hf age is caused by very limited spread in $^{176}\text{Lu}/^{177}\text{Hf}$ ratios (0.7). Similarly the metapelite garnet from N. Vietnam was strongly affected by inclusions and yielded $^{147}\text{Sm}/^{144}\text{Nd}$ ratios too low to determine an age. Metapelite garnets, which were very rich in monazite, zircon and apatite inclusions, were subjected to leaching experiments.

We modified the leaching procedure of Amato et al. (1999). Two leaching steps with concentrated HF, followed by 6N HCl yielded $^{147}\text{Sm}/^{144}\text{Nd}$ ratios of 0.97 and 1.08, respectively. The remaining residue gave a low Sm/Nd ratio due to strong contamination by inclusions undissolved at earlier steps (as indicated by a very high Nd concentration). Two other garnet fractions from the same sample treated with concentrated H_2SO_4 and subsequently fully dissolved gave identical, very high $^{147}\text{Sm}/^{144}\text{Nd}$ of 1.97.

All points from both experiments plotted on a single errorchron of age 41.8 ± 4.3 Ma (MSWD = 3.4 and probability of fit = 0.02). The poor statistics are caused by the HF leachate analysis, during which some Nd was leached from inherited monazite and zircon inclusions. After removing this point from the regression an isochron age of 41.7 ± 1.5 Ma is obtained with MSWD = 0.057 and probability of fit = 0.94.

Our data demonstrates that H_2SO_4 leaching can effectively remove phosphate inclusions enhancing precision and reliability of Sm-Nd garnet chronology.

References

- Amato, J.M., Johnson C.M., Baumgartner L.P., Beard B.L., (1999) *Earth Planet. Sci. Lett.* **171**, 425-438.
Thirlwall, M.F., (1988) *J. Geol. Soc. London* **145**, 951-967.

Geochemistry and Geochronology of Basement Rocks from the Pelagonian Zone, Greece

B. ANDERS^{1,2}, T. REISCHMANN^{1,2} AND U. POLLER²

¹ Dep. of Earth Sciences, Johannes Gutenberg-University, Mainz, Germany (banders@mail.uni-mainz.de)

² Max-Planck-Institut of Chemistry, Dep. of Geochemistry, Mainz, Germany

The Pelagonian Zone forms a major crustal entity within the Central Hellenides. It is located between the Serbomacedonian Massif and the Rhodope Massif (Internal Hellenides) to the east and the Pindos Zone (External Hellenides) to the west. The prevailing rock types of the Pelagonian Zone are granitic and minor mafic gneisses, presumably Mesozoic carbonates, ophiolites and Palaeocene Flysch.

In our study we concentrated on basement rocks, especially on the orthogneisses. These orthogneisses show variable deformation ranging from almost undeformed rocks with a granitic texture to highly sheared gneisses. Augengneisses are common with feldspar "augen" up to several centimeters in size. Despite their variable deformation the ages of the rocks are rather homogenous indicating a Permo-Carboniferous crust-forming event at 280-300 Ma. These ages were obtained by single zircon analysis using the Pb/Pb evaporation technique and were later confirmed by single zircon U-Pb-dating. Cathodoluminescence imaging of the zircons from the dated samples showed the magmatic oscillatory zoning indicating an igneous origin of these zircon grains.

Based on the geochemical composition the orthogneisses are classified as Syenogranite, Monzogranite or Granodiorite, only some are Monzodiorites and Monzogabbros. Using geochemical parameters such as the Fe*-number, the aluminium saturation index and the modified alkali index most of the basement rocks are characterized as slightly peraluminous and magnesian. They belong to an alkalic-calcic to calcic suite. Based on the low concentrations of HFSE such as Nb and Y the granitoid rocks of the Pelagonian Zone are identified as volcanic arc or collisional granitoids.

Sr isotope analysis gave $^{87}\text{Sr}/^{86}\text{Sr}_{(300)}$ initial ratios ranging from about 0.703 to 0.705. Such low Sr ratios indicate a mantle source, from which the magmas were derived, such as the depleted mantle with only small contributions of older continental crust. The geochemical and isotopic data support the model that the basement rocks of the Pelagonian Zone formed as part of a magmatic arc in a subduction zone environment during the Upper Carboniferous/Lower Permian.

The Mesoproterozoic continental margin of the Baltic Shield: Geochemical evidence for a Cordillera-type setting

T. ANDERSEN¹ AND W.L. GRIFFIN²

¹Department of Geology, University of Oslo, PO Box 1047 Blindern, N-0316 Oslo, Norway (tom.andersen@broadpark.no)

²GEMOC Key Centre, Earth and Planetary Sciences, Macquarie University, NSW 2109, Australia

The evolution of the mid-Proterozoic, southwestern continental margin of the Baltic Shield has been much debated recently. A central issue is whether the Precambrian crust of SW Sweden and S Norway evolved as part of a single continental margin, or if the westernmost part of the area (i.e. parts of present-day S Norway) is an exotic microcontinent with a separate history, accreted onto the Baltic Shield between 1.6 and 1.5 Ga (e.g. Åhäll et al. 2000, Andersen et al. 2001). Mesoproterozoic, subduction-related metaigneous rocks are widespread in the area, and provide an important test of the age and character of the subduction zone(s) involved. If such rocks on either side of potential sutures show the same timing, tectonic setting and source material, it is strong evidence against tectonic models which claim the presence of rocks of non-Baltic Shield origin in the area.

The U-Pb and Lu-Hf systematics of zircons from Proterozoic metaintrusive calcalkaline gneiss complexes across south Norway have been studied by laser-ablation microprobe ICPMS. U-Pb data from populations of single zircons suggest that most intrusions were emplaced between 1.61 and 1.55 Ga, and some intrusions are distinctly younger (down to 1.51 Ga). There is no systematic distribution of ages with respect to potential suture zones, suggesting the presence of a single, long-lived (100-160 Ma) subduction zone system in the area. Initial Hf isotopic ratios change gradually from juvenile values in the westernmost (most distal) complexes ($\epsilon_{\text{Hf}} = +13$) to $\epsilon_{\text{Hf}} = +6$ in the eastern areas, where the presence of a 1.6-1.7 Ga basement is demonstrated by inherited zircons. The calcalkaline intrusions in S Norway show the major and trace element characteristics of intrusive rocks formed in a moderately evolved magmatic arc at a continental margin, and represent a more evolved stage of an arc evolution that may have started with eruption of low-K mafic volcanic rocks of the Stora-Le Marstrand belt in SW Sweden and their possible equivalents in S Norway. The data from south Norway contradict the hypothesis of an exotic microcontinent in S. Norway and of a 1.5-1.6 Ga continental collision event at the SW margin of the Baltic Shield. The NW American Cordillera may be a useful analogue for the tectonomagmatic evolution of the mid-Proterozoic Baltic margin.

References

- Åhäll, K.-I., Connelly, J. and Brewer, T.S. (2000), *Geology* **28**, 823-826.
 Andersen, T. Andresen, A. and Sylvester A.G (2001): *J. Geol. Soc. Lond.* **158**, 253-267.

Glacial-Interglacial Variability in the Accumulation of Lithogenic material in Central Equatorial Pacific Sediments

R. F. ANDERSON AND M. Q. FLEISHER

Lamont-Doherty Earth Observatory, Columbia University, Palisades, NY, USA 10964 (boba@ldeo.columbia.edu)

Records from ice cores, and from marine sediment cores in many regions, have led to the view that the world was "dustier" during glacial periods than during interglacials. Recent modeling efforts support this view. Reconstructions from sediments in the eastern and central equatorial Pacific Ocean depart from this pattern, however. Previous investigators have concluded either that maximum dust deposition occurred during interglacials, or that there is no systematic relationship between climate state and dust flux to the region. Either the climate-related variability in supply of eolian material to this region has not been in phase with the rest of the world, or unrecognized factors have influenced the evaluation of eolian fluxes to equatorial Pacific sediments.

Here we report accumulation rates of lithogenic material from a transect of cores crossing the equator at 140°W, evaluated by normalizing to ²³⁰Th to correct for sediment focusing and to overcome biases associated with subtle errors in chronology. Titanium and ²³²Th are used as proxies for lithogenic material, each providing unique information; e.g., ²³²Th is enriched in continental crust but depleted in ocean basalts. These records show a coherent pattern of ²³²Th accumulation among the cores, including: 1) a positive correlation between ²³²Th accumulation and ice volume, as inferred from benthic foraminiferal ¹⁸O; 2) a maximum amplitude of about a factor of two in the climate-related variability in ²³²Th accumulation; and 3) average ²³²Th accumulation rates that decrease systematically from north to south across the equator. In contrast to ²³²Th, accumulation of Ti shows no detectable climate-related variability in the two records with greatest temporal resolution (Eq. and 2°S), reflecting the different sources of Th- and Ti-bearing lithic material. To the extent that ²³²Th accumulation traces primarily the supply of old continental crustal material, these results indicate a pattern of dust supply to the central equatorial Pacific Ocean similar to that observed in most other regions.

Preeruptive Sizes of Bubbles in Bishop Tuff Rhyolitic Magma

ALFRED T. ANDERSON, JR.

Department of the Geophysical Sciences, The University of Chicago, 5734 S. Ellis Ave., Chicago, Illinois, 60637, USA (canderso@midway.uchicago.edu)

CO₂ dissolved in glass inclusions in quartz phenocrysts decreases with differentiation, and this relationship has been interpreted to reflect gas-saturated crystallization. However, bubbles of gas are virtually absent in rapidly cooled glass inclusions in Bishop quartz phenocrysts. If pre-eruptive bubbles were much smaller than glass inclusions, then they should be present in the glass inclusions. Therefore, pre-eruptive bubbles plausibly were too large to be captured in glass inclusions, and the glass inclusions are smaller than about 0.4mm diameter. Bubbles enclosed within reentrants and hourglass inclusions are up to about 0.1mm diameter, and this indicates that bubbles as large as about 0.06mm (before decompressive expansion) might be trapped within totally enclosed glass inclusions that formed in the Bishop magma. Pumice clasts contain vesicles that are up to about 10mm in diameter and commonly several mm in diameter. Textures of bubble-bearing hourglass inclusions and H₂O concentrations in glassy reentrants suggest that the pressure at which the vesicles stopped expanding is several hundred atmospheres. Therefore the decompressive enlargement of the pre-eruptive bubbles during eruptive ascent is by a factor no greater than about 10 by volume or about 2 by diameter. Evidently a 10mm diameter bubble quenched at 300 atm would be about 5.8 mm diameter at 1500 atm. Taking account of H₂O exsolution during bubble growth only further diminishes the inferred maximum size of pre-eruptive bubbles. Thus the pre-eruptive bubbles are evidently smaller than about 6mm in diameter. Although questions about selective preservation of small inclusions, mechanisms of hourglass formation and a possible role of surface tension gradients allow some uncertainty, the pre-eruptive sizes of bubbles that accompanied crystal growth in the Bishop magma can thus be constrained to lie between about 0.06mm and 6mm in diameter.

10,000 year nitrogen isotope record from Lake Ontario, understanding carbon and nitrogen dynamics from a paleo-perspective

W.T. ANDERSON¹, M.A. MCFADDEN², H.T. MULLINS², AND W.P. PATTERSON²

¹Earth Science Dept./SERC, Florida International University, Miami, FL 33133, USA

²Dept. of Earth Sciences, Syracuse University, Syracuse, NY 13244, USA

In order to understand future changes in trophic levels in lakes, it is important to investigate the paleolimnologic records from different basins. Paleo-investigations can give insight through proxy records of productivity and ecological changes throughout a lake's evolution. Here we present an isotopic investigation of the organic matter (OM) preserved in the last 10ka from the Rochester Basin, eastern Lake Ontario. A series of piston cores were collected in June of 2000, from which two cores were used to construct a composite sedimentary record (cores LO-1 and LO-3). The entire composite record is 514 cm long, where the upper 420 cm consists of a grey-brown laminated mud, which is underlain by a massive brown mud (421 to 514 cm).

Nitrogen isotopic analyses were measured on whole sediment samples, whereas carbon isotopic analyses were only measured on decarbonated samples. Additional supporting analyses were also carried out on the core including: magnetic susceptibility, total OM, total carbonate, biogenic silica and C/N ratios. Isotopic analyses were measured on 2 cm intervals, yielding a relatively high-resolution record. The $\delta^{15}\text{N}$ values ranged from 3.0‰ to 7.5‰, with an average of 4.2‰. The highest $\delta^{15}\text{N}$ values occurred in the upper 10cm of the core, representing recent anthropogenic forcing. The nitrogen isotopic record also displays up to 6 sub-millennial scale enrichment-depletion cycles of up to 1‰. C/N ratios indicate that a majority of the preserved OM in the core consists of lacustrine phytoplankton with values less than 12. Additionally these data indicate that the degree of N-limitation has changed over the last 10ka. The nitrogen isotopic data also displays a unique decoupling from the carbon isotope data, indicating that changes in primary production and/or nutrient limitation have occurred back in time. Further work is being carried out on linking climate change to the natural variability of Lake Ontario's trophic state.

Evolution of the depleted asthenosphere beneath the Atlantic: Evidence from ϵHf in N-MORB from 80°N to 55°S

MAGDALENA ANDRES¹, JANNE BLICHERT-TOFT² AND JEAN-GUY SCHILLING¹

¹ Graduate School of Oceanography, University of Rhode Island, Kingston, RI, 02881 (mandres@gis.net, jgs@gso.uri.edu)

² Ecole Normale Supérieure de Lyon, 69364 Lyon Cedex 07, France (Janne.Blichert-Toft@ens-lyon.fr)

ϵHf in N-MORB with $(\text{La}/\text{Sm})_n < 0.65$ from 12 different "normal" ridge segments remote from plume/ridge interactions, exhibit a striking linear gradient along the entire 15,000 km long Mid-Atlantic Ridge (MAR) from 80°N to 55°S . ϵHf decreases from +23.9 in the Arctic to +13.4 near the Bouvet Triple junction in the South Atlantic. Similar gradients are also apparent in $^{207}\text{Pb}/^{204}\text{Pb}$ and to a lesser extent ϵNd . ϵHf correlates negatively with MAR spreading rate and with distance between the MAR and the continents. There is no correlation between ϵHf and ridge depth, age of Atlantic opening or Lu/Hf . The inverse relationship between spreading rate and ϵHf indicates that the observed Atlantic isotope gradients are not caused by differences in efficiency of melt collection from the "wings" of the melt zone in a mantle containing enriched veins or blobs. The isotope gradients may be caused by pollution from continental lithosphere delaminated during Atlantic opening. However, the negative correlation of ϵHf with MAR-continent distance indicates that such a lithosphere pollutant has been incompatible element depleted for a long time. It is also possible that the Atlantic mantle is polluted by residues of fractional melting associated with plume dispersal. Finally, it is possible that the gradients are not related to any pollutant (veins/blobs, continental lithosphere or plume residues) but are due to longstanding variations related to the evolution of the depleted upper mantle. In this case, the mantle underlying the Atlantic has been more incompatible element depleted toward the north due to a greater extent of melt/fluid removal through time in forming continents. Alternatively, the depletion of the upper mantle by melt removal and continent formation may have begun earlier in the north than in the south resulting in an older mean age for the northern upper mantle. However, any of these inherent upper mantle variations must be ancient to allow for radiogenic ingrowth. Thus they predate the opening of the Atlantic and must have developed during the formations and breakups of earlier continents.

High-resolution, Southern-Hemisphere record of rapid climate change at Termination I and subsequent cold reversal: Great Australian Bight, ODP Leg 182

M. S. ANDRES, S. M. BERNASCONI, J. A. MCKENZIE

Geological Institute, ETH-Zentrum, 8092 Zurich, Switzerland (andres@erdw.ethz.ch)

The transition from the last glacial maximum to the Holocene was by no means smooth and continuous but was marked by several rapid climate fluctuations, as indicated by a stepwise rise in sea-level. High-resolution and well-dated marine records from the Southern Hemisphere are rare, yet they would be important for our understanding of the last glacial cycle on a global scale. We used a marine sediment core recovered during ODP Leg 182 on the Great Australian Bight to reconstruct the deglaciation history of this geographic realm.

Site 1127 is situated on the continental shelf facing the open ocean in a mid-latitude Southern-Hemisphere location. The simultaneous deposition of surface-dwelling planktonic foraminifera together with the benthic shelf community makes the sedimentary record deposited in this region sensitive not only to paleoceanographic but also to environmental changes affecting the shelf. Study of this combined record permits us to link changes in the open-ocean with those occurring in the continental-margin setting. High sedimentation rates and well-preserved foraminifera enabled us to develop a high-resolution oxygen isotope stratigraphy for the evaluation of the paleoceanographic changes. A detailed AMS C-14 chronology is used to determine the relative timing of sea-level rise and climatic fluctuations and compare these with other paleoclimatic records.

Our isotope data indicate abrupt warmings at 16.5 and 14 cal yr B.P. that can be associated with large sea-level rises observed in regional and global records. A rapid return to cooler sea-surface temperatures, dated between 12.3 and 11 cal yr B.P., points to an abrupt end to the deglaciation. Overall, mass accumulation rates increase from the Late Glacial to the Holocene as sea-level rises, flooding the shelf and reinitiating cool-water carbonate production.

We compare the relative timing of Termination I and subsequent rapid cold reversal with regional climatic records, as well as Greenland and Antarctic ice-core data. The rapid cold reversal observed in the Great Australian Bight between 12.3 and 11 cal yr B.P. supports the Oceanic Cold Reversal hypothesized by Stenni et al., 2002. Interestingly, this cooling is quasi-synchronous with the "Younger Dryas Event" in Europe (12.6-11.5 cal yr B.P.)

Reference

Stenni B. et al., (2002), *Science* **293**, 2074-2077.

The Late Silurian Lau Event: isotopic evidence for causes of extinction

A.S. ANDREW¹, D.J. WHITFORD², L. JEPSSON³, J.A. TALENT⁴, R. MAWSON⁴ AND A. J. SIMPSON⁴

¹ CSIRO Exploration & Mining, PO Box 136 North Ryde 1670, Australia (anita.andrew@csiro.au)

² CSIRO Petroleum Resources, PO Box 136 North Ryde 1670, Australia (david.whitford@csiro.au)

³ Department of Geology, Solvegatan 13, SE 223 62 Lund, Sweden (lennart.jepsson@geol.lu.se)

⁴ Macquarie University Centre for Ecostratigraphy and Palaeobiology, Department of Earth and Planetary Sciences, Macquarie University 2109, Australia (jtalent@els.mq.edu.au; rmawson@els.mq.edu.au; asimpson@els.mq.edu.au)

The Silurian sequences of Gotland (Sweden), the Broken River region of NE Australia, were located on different palaeocontinents, the first on Baltica, the other on the N Gondwana margin. Though faunal differences are evident, conodonts are of prime importance for correlating the stratigraphies and identifying the Lau Event in the two regions. The Lau Event affected, *inter alia*, acritarchs, corals, polychaetes, brachiopods, chitinozoans, ostracods, trilobites, tentaculites, graptolites, conodonts and fish. Imprecise knowledge of range-ends hampers quantitative evaluation of extinctions but a loss of at least 30 to 50 % of the species seems probable. Among higher taxa, the event caused extinction of a suborder of tabulate corals. Among conodonts, no platform-equipped taxon survived but 24 of the 34 species known to have persisted until the beginning of the event survived.

The sequence of lithologies is remarkably similar on Gotland (Sweden) and from the coral gardens section (COG) of the Jack Formation, North Queensland: A. argillaceous strata before the event; B. more weathering-resistant limestones during the early part of the event; C. oncoids and crinoids (oncolitic crinoid limestone or oncolite with crinoids) during the middle part of the event; D. argillaceous oncolite during the late part of the event, and then E. terrigenous clastics followed by F. oolite before G. return in each area to normal sediments.

Isotopic changes are very similar in both regions indicating globality of changes in ocean chemistry. The $\delta^{13}\text{C}_{\text{carb}}$ record includes a slow rise during A, a slightly more rapid rise during B, an abrupt (a few hundred years or less) shift upwards of >1‰ during 3 000-4 000 years before the lithologic change at B/C, a rapid rise initially during C, stable high values during D, an abrupt shift downwards at the start of E, followed by a rapid rise. In the detailed section through the coral gardens section (COG), C (carbonate, organic C), Sr and O isotope records indicate changes in ocean chemistry leading up to the event and in its aftermath. The relative timing of isotopic, lithological and faunal change give insight into the mechanisms driving the global change.

Silicic melt generation by basalt crystallization in the deep crust

C. ANNEN¹, R. S. J. SPARKS², J. BLUNDY³

University of Bristol, Dpt of Earth Sciences, Wills Memorial Building, Queens Road, Bristol, United-Kingdom
(¹ c.j.annen@bristol.ac.uk, ² steve.sparks@bristol.ac.uk, ³ Jon.Blundy@bristol.ac.uk)

The thermal evolution of the crust when repeatedly invaded by basaltic sills was simulated numerically. A thermal anomaly progressively builds up as sills solidify and transfer their heat to the surrounding rocks. Eventually the solidus temperature is exceeded and melt starts to accumulate. The duration of the incubation period before the outset of melt accumulation depends on the magma intrusion rate and on the initial temperature of the crust. For example, with a 20°C km⁻¹ geothermal gradient, an intrusion depth of 20 km and a magma intrusion rate of 50 m per 10,000 years, the incubation period is of 3x10⁵ years. Melt is generated simultaneously by incomplete crystallization of the fresh basalt, by remelting of formerly intruded basalt and by partial melting of the pre-existing old crust. The proportion of different melt sources depends on the configuration of the sills, on the fertility of the crust and on the water content and temperature of the injected basalt. For typical arc-type basalt injected at 1100°C and containing 2.5% water, most melt is generated by crystallization of the basalt itself. The intrusion of one 50 m sill every 10,000 years at 30 km depth during 3.2 millions years results in a partially molten layer 16 km thick. The melting degree ranges from 20 to 25% corresponding to an equivalent pure melt thickness of 3600 m. Comparison with experimental data indicates that the melt is dacitic to rhyolitic in composition. Part of the water originally present in the basalt is trapped in residual or cumulate amphiboles. The remaining water concentrates in the melt. Assuming 30% amphiboles trapping a total 0.6% of the water, the water concentration in the melt exceeds 8.5%. Because of this high water content, the melt viscosity is only 10³-10⁴ Pa s. Another effect of high water concentration is to decrease the melt density substantially. The low density and viscosity of these water-rich silicic melts promotes segregation of melt by compaction and Rayleigh-Taylor instabilities in the zone of partial melting. Subsequent ascent of this melt will be very rapid. These melts degas and crystallize when they ascend into the upper crust.

Tonalite generation in arc regimes: results from metadiorite partial melting experiments

A. ANTIGNANO IV AND T. RUSHMER

Department of Geology, University of Vermont, Burlington, VT, 05405, USA (aantigna@zoo.uvm.edu)

Piston-cylinder experiments have been conducted to determine the melt composition, volume change of the melting reactions and the aH₂O of melt produced during partial melting of a metadiorite. An unmelted sample of metadiorite (plag + qtz + hbl + bt + czo) was collected from the Pembroke Valley, Fiordland, New Zealand. The metadiorite experienced partial melting simultaneously with fracturing at granulite facies conditions T>750°C and P~1.4 GPa during the Early Cretaceous (Clark et al., 2000).

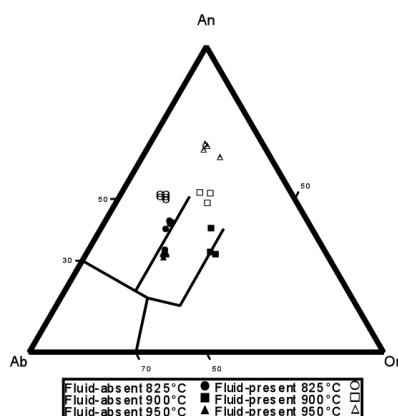
Fluid-absent Results

The fluid-absent solidus occurs between 800-825°C. Experimental melt compositions are presented in Figure 1. Low T melts suggest the initial reaction of bt followed the partial melting of hbl +/- czo. Cpx, grt and melt are the primary reaction products. Melt compositions are initially tonalitic but become granodioritic with T, as grt becomes stable and the dominant reaction shifts to hbl +/- czo. Compositions later become more tonalitic as more czo is incorporated into the melting reaction. The hbl + czo reaction has a positive ΔV, producing melt filled cracks and suggests a high dilatational strain is associated with melting. LA-ICPMS data show that 950°C melts are adakitic.

Fluid-present (2wt% H₂O added) Results

The solidus under these conditions occurs between 750-800°C. The melt compositions reflect a similar evolution as in the fluid-absent experiments. Increased Ca concentrations as a function of T are attributed to the early involvement of czo in the melting reaction, the absence of product grt, and hbl remaining stable in excess of 950°C.

Figure 1: 1.4 GPa experimental melt compositions.



References

Clarke, G.L., K.A. Klepeis, and N.R. Dazcko. (2000), *JMG.*, 18, 359-374.

Interannual variability of the POC export flux estimated from Th-234 in the equatorial Pacific during the period 1999 to 2001

TATSUO AONO AND MASATOSHI YAMADA

Research Center for Radiation Safety, National Institute of Radiological Sciences, Ibaraki, JAPAN (taono@nirs.go.jp, m_yamada@nirs.go.jp)

Introduction

The boundary of the warm pool and the upwelling area is dependent on the east-west advection of the western Pacific warm pool in the equatorial Pacific. The change of boundary also affects the carbon productivity by biomass and the transport process of carbon in this area. It is important to clarify the carbon export flux in order to understand the carbon cycling mechanism in the upper ocean. Th-234 ($t_{1/2}$ =24.1 day) was used as a tracer to investigate the scavenging and export fluxes of particle transport processes. The export fluxes of POC were estimated from Th-234 in the western and central equatorial Pacific during 1999 to 2001. Seawater and settling particle samples were taken from the surface to the depth of 200m during MR98-K02, MR99-K07 and MR00-K08 cruises, aboard the R. V. Mirai of JAMSTEC.

Results and Discussion

The surface water temperature tended to lower from the west to the east in the equatorial Pacific. The boundary in the warm pool in the western Pacific and the upwelling area in the equatorial Pacific was recognized near 155-160E. In the upwelling area, there was no correlation to the Chl. a and POC concentrations in seawater. It has been clarified to be a result by the difference between the species of plankton (Matsumoto et al., 2001).

The ratios of POC in the settling particles could not recognize the large difference in this area. The POC/Th-234 ratios in the suspended particles showed the value in which 2 times were higher than those in the settling particles. The export fluxes of POC were calculated as the product of the calculated flux of Th-234 in seawater times the POC/Th-234 ratio in the settling particles. Measured POC export fluxes in the depth of 200 m were from 1.1 to 10.0 mmolC/m²/day and estimated export fluxes of POC ranged from 1.0 to 8.2 mmolC/m²/day. The e ratios (the ratio of POC export flux in primary production) were from 0.03 to 0.27. These ratios showed that the values in the warm pool were higher than those in the upwelling area. It is considered that the different of the POC export flux and the e ratio in these areas are attributed to cause by the compositions of particle matter and the plankton species.

References

Matsumoto K., Kawano T. and Asanuma I., (2000) 2000 Fall Meeting of Oceanogr. Soci. of Japan Abs., pp.223.

Alkylphenols and light aromatic hydrocarbons in oilfield waters are produced in source rocks, not from petroleum hydrolysis

A.C. APLIN, G.D. LOVE, J.D. DALE, B. BENNETT, G. TAYLOR AND S.R. LARTER

NRG, University of Newcastle, Newcastle upon Tyne, NE 1 7RU, UK

Diverse experimental, theoretical and empirical evidence has recently been used to suggest that metastable, thermodynamic equilibrium may be attained between oil, water, CO₂ and rock minerals in sedimentary basins. Here, we present evidence which we believe shows that the concentration and distribution of low molecular aromatic hydrocarbons (BTEX: benzene, toluene, ethyl benzene and xylene) and alkylphenols in oilfield waters are not interrelated through redox and hydrolysis reactions. Rather, the concentrations and distributions of BTEX and alkylphenols in oils are inherited from the pattern of compounds generated from kerogen. The distribution of BTEX and alkylphenols in oilfield waters simply represents partition equilibrium between oil and water. The key evidence which favours this simple hypothesis includes:

1. Similar distributions of alkylphenols in source rock extracts and oils
2. Similar distributions of alkylphenols in oils and pyrolysates of source rock kerogen
3. Abundances of alkylphenols and BTEX in oilfield waters which are consistent with partition equilibrium between oil and water, using laboratory measured partition coefficients
4. GC-C-IRMS data which show that phenol in both oil and water is ¹³C-enriched by up to 7-8‰ in comparison with coexisting BTEX, which in turn have isotopic compositions which are similar to bulk oil. Bound phenol in source rock kerogen is also significantly isotopically heavier than the corresponding bulk TOC, implying a different source, perhaps carbohydrate or protein moieties.

At least for BTEX and alkylphenols, we suggest that reversible chemical reactions controlled by master geochemical variables such as fO_2 do not appear to be important at the temperatures of most oilfields. Rather, characteristics inherited from the source rock dominate the observed distributions.

Use of geochemical and isotope tools to evaluate nitrate attenuation in riparian wetlands in agricultural landscape in Southern Ontario

R. ARAVENA, C. BROWN, S.L. SCHIFF AND R. ELGOOD

Department of Earth Sciences, University of Waterloo,
Canada (roaraven@sciborg.uwaterloo.ca;
sschiff@sciborg.uwaterloo.ca;
rjelgood@sciborg.uwaterloo.ca)

Introduction

Nitrate contamination associated with agricultural activities is a major problem in shallow aquifers in Canada and is becoming an increasing threat to groundwater supplies and surface water quality. Riparian zones (buffer strips and wetlands) located at the interface between groundwater-surface water appears to have an inherent ability to naturally attenuate nitrate derived from agricultural sources. The attenuation capacity of riparian zones is linked to a complex interaction between hydrogeological, geochemical and biological conditions. This presentation will focus on research carried out in 5-ha cedar swamp that drains into a lake reservoir. The wetland is fed by nitrate contaminated groundwater originating in upstream agricultural areas. A detailed hydrogeological and geochemical investigation was conducted at the study site.

Results and Discussion

The aquifer is mainly composed of silty sand overlain by organic rich sediments and underlying by clay sediments. However, at a small scale, a significant spatial variability is observed in hydraulic conductivity. The nitrate input in the upstream areas of the wetland range between 16 and 10 mg/L as nitrogen. A significant spatial variability is observed in the nitrate behavior in different parts of the wetland. A general nitrate trend shows a significant drop in concentration to values as low as 1 mg/L along the groundwater flow system toward the lake. Oxygen and dissolved organic carbon concentration patterns suggest that denitrification is the main mechanism responsible for nitrate attenuation at the study site. This is confirmed by $\delta^{15}N$ and $\delta^{18}O$ data in nitrate that show the expected trend for denitrification, an enrichment in the isotope composition of the nitrate as the nitrate concentration decreases. The main findings of this study will be compared with other nitrate studies that we have conducted in other riparian zones in Southern Ontario. Our research demonstrate that studies of nitrate attenuation in riparian zones requires a detailed evaluation of the groundwater flow system and groundwater geochemistry.

Large fractionations in Fe, Cu and Zn isotopes associated with Archean microbially-mediated sulphides

C. ARCHER AND D. VANCE

Department of Geology, Royal Holloway, University of London, Egham, Surrey TW20 OEX, U.K.
(c.archer@gl.rhul.ac.uk, d.vance@gl.rhul.ac.uk)

Perhaps the most important potential application of transition metal isotope geochemistry is in the study of biogeochemical processes, particularly early in Earth history where morphological evidence for life is rare, equivocal or absent. Early studies have shown that biological systems consistently use the lighter isotopes preferentially. Given the potential for non-biological fractionation of the transition metals, however, the greatest degree of success in utilising these systems will probably come from a multi-isotopic approach. Here we present a combined Fe-Cu-Zn isotopic dataset from sulphide grains and black shales from the 2.7Ga Belingwe Belt, Zimbabwe, associated with sulphate-reducing microbial communities.

We have tested these techniques using analyses of USGS basalt BCR-1. In common with previous studies of Fe (Beard and Johnson 1999) and Zn (Marechal et al. 2000) isotopes in terrestrial basalts we have observed very small fractionations for this sample. We have measured $\delta^{56}\text{Fe}$ of $+0.11 \pm 0.04$ ‰, $\delta^{66}\text{Zn}$ of 0.2 ± 0.06 ‰ and $\delta^{65}\text{Cu}$ of 0.1 ± 0.06 ‰ (relative to IRMM-14 Fe, Lyons JMC Zn and NIST 976 Cu respectively).

In contrast, organic-carbon-rich black shales from Belingwe exhibit extreme depletions in heavy Fe and Cu isotopes relative to IRMM-14 and NIST 976 – with $\delta^{56}\text{Fe} = -2.9$ ‰, $\delta^{65}\text{Cu} = -1.0$ ‰. Zinc isotopes exhibit positive fractionations in the black shales – $\delta^{66}\text{Zn} = +1.1$ ‰. 15 individual sulphide grains from the same section spread along correlations between BCR-1 and the Belingwe black shales, with $\delta^{56}\text{Fe}$ exhibiting a range of -1.2 to -2.7 ‰, $\delta^{65}\text{Cu}$ varying between -0.1 and -1.0 ‰ and $\delta^{66}\text{Zn} = +0.3$ to +1.1 ‰. Furthermore, these data are correlated with depletions in ^{34}S of up to 18 ‰ (Grassineau et al. 2001). The negatively skewed nature of the Fe isotopic dataset, in combination with the positive Zn (cf. Marechal et al. 2000) and negative Cu, strongly suggest involvement of biological processes. However, fractionation of Fe isotopes is not, *a priori*, expected during microbially-mediated sulphide precipitation itself but probably reflects the operation of repeated reduction and re-oxidation cycles.

References

- Grassineau N.V. et al., (2001) *Proc. Roy. Soc. London B* **268**, 113-119.
Maréchal C. N. et al., (1999), *Chem. Geol.* **156**, 251-273.
Maréchal C. N. et al., (2000), *G-cubed* **1**, 1999GC000029.
Beard B. L. and Johnson C. M., (1999), *Geochim. Cosmochim. Acta*, **63**, 1653-1660.

Geochemical model of the granite-bentonite-groundwater at Äspö (LOT experiment)

D. ARCOS¹, J. BRUNO¹ AND O. KARNLAND²

¹ ENVIROS, Parc Tecnològic del Vallès, Cerdanyola del Vallès 08290 Spain (darcos@quantisci.es, jbruno@quantisci.es)

² Clay Technology AB, IDEON Research Center S-223 70 Lund, Sweden (ok@claytech.se)

In the nuclear waste repository designed by SKB, bentonite is considered as a barrier between the geologic environment and the canister containing the spent nuclear fuel. The use of bentonite as a barrier has a double motivation. First, it isolates the nuclear waste from groundwater due to its swelling capacity as it saturates with water. Second, in case the isolation fails, it could retard the radionuclide migration outside the system due to its sorption capacity on the clay surface.

In this context, it is very important to know how bentonite responds to some geochemical processes, which are likely to occur in an underground repository. For this reason, SKB financed the LOT experiment in Äspö, Sweden (Karnland et al., 2000). The aim of this experiment is to understand how bentonite reacts to changes produced by a thermal gradient and/or to the addition of some substances at different bentonite blocks, such as NaCl, KCl, gypsum, calcite, and cement, among others.

We modelled some of the special cases of the LOT experiment. The calculations were performed using a two-dimensional reactive-transport model with the code PHAST (Parkhurst et al., 2000). The results indicate that calcite is buffering pH in almost all cases, except where cement is present. In this case the equilibrium with portlandite implies a very alkaline pH and the precipitation of sulphides leads to reducing conditions. The calcite dissolution-precipitation is governed by the calcium in solution, which is mainly controlled by the cation exchange in the bentonite. The effect of adding KCl or NaCl to the bentonite results in an acidification of the solution. This is because Ca in solution increases due to the cation exchange, leading to a large precipitation of calcite.

Acknowledgements: This work has been financed by SKB.

References

- Karnland O., Sandén, T., Johannesson L.E., Eriksen T.E., Jansson M., Wold S., Pedersen K., Motamedi M. and Rosborg B. (2000) SKB Tec. Rep. TR-00-22, 131 pp.
Parkhurst D.L., Kipp K.L. and Engesgaard P. (2000) PHAST.A Program for Simulating Ground-Water Flow and Multicomponent Geochemical Reactions. User's guide. USGS, 154 pp.

Reconstructing greenhouse-gas history from the plant fossil record: Examples from the Cretaceous

NAN CRYSTAL ARENS¹ AND A. HOPE JAHREN²

¹ Department of Geosciences, Hobart & William Smith Colleges, Geneva, New York USA (arens@hws.edu)

² Department of Earth and Planetary Sciences, Johns Hopkins University, Baltimore, Maryland USA (jahren@jhu.edu)

Fluctuating levels of greenhouse gasses alter the carbon isotope composition ($\delta^{13}\text{C}$) of atmospheric carbon dioxide. Terrestrial land plants sample atmospheric CO_2 during photosynthesis, thus their fossil record offers an isotopic composite of paleo-atmospheric $\delta^{13}\text{C}$ value. Here, we infer changing $\delta^{13}\text{C}$ values of the paleo-atmosphere using fossil plant tissue during two intervals of the Cretaceous and test quantitative hypotheses about greenhouse gas sources.

$\delta^{13}\text{C}$ values of Land Plants and Atmospheric CO_2

For C_3 plants, the $\delta^{13}\text{C}$ value of plant tissue is a function of the isotope composition of the CO_2 fixed, less discrimination by diffusion, enzyme preference, and the balance between carbon gain and water loss. A meta-data set including 519 carbon isotope measurements made on 176 living species showed a strong, significant relationship between the $\delta^{13}\text{C}$ values of plant tissue and the $\delta^{13}\text{C}$ values of the atmosphere under which it was fixed. This analysis provided quantitative confidence estimates for paleo-atmospheric carbon isotope reconstructions (Arens et al., 2000).

Actualistic tests demonstrated the accuracy of the method (Arens et al., 2000) and showed that the $\delta^{13}\text{C}$ value of plant tissue was not systematically biased by depositional environment (Arens and Jahren, 2000).

Examples from the Cretaceous

Sites in North and South America reveal a global negative isotope excursion between ~3-8‰ during the Aptian. Mass balance calculations suggest methane hydrate as a likely source of the added carbon (Jahren et al., 2001).

At the Cretaceous-Tertiary (K/T) boundary, we observe a -2‰ excursion at localities where the boundary is diagnosed by Ir and shocked minerals. The excursions magnitude and brief duration ($\approx 100,000$ yrs.) suggest multiple carbon sources (Arens and Jahren, 2000).

References

- Arens N.C. and Jahren A.H. (2000) *Palaios* 15, 314-322.
 Arens N.C., Jahren A.H. and Amundson R. (2000) *Paleobiology* 26, 1137-164.
 Jahren A.H., Arens N.C., Sarmiento G., Guerrero J. and Amundson R. (2001) *Geology* 29, 159-162.

Unraveling an orogenic core: isotopic studies on the western syntaxis of the Himalaya

T.W. ARGLES¹ AND G.L. FOSTER²

¹ Department of Earth Sciences, The Open University, Walton Hall, Milton Keynes MK7 6AA, UK (t.w.argles@open.ac.uk)

² Department of Geology, Leicester University, Leicester, LE1 7RH, UK (glf3@leicester.ac.uk)

Isotopic tectonostratigraphy

The western Himalayan syntaxis (Nanga Parbat massif) is a typical example of an orogenic core region in its frequent intractability to conventional tectonic mapping and correlation with the bulk of the Himalayan orogen to the east. High strain and Neogene metamorphic events in particular prevent easy correlation of tectonic units that is otherwise possible along the length of the Himalayan arc. Whittington et al (1999) showed that gneisses in the core of the syntaxis, generally assigned to the High Himalayan Crystalline Series (HHCS) on the basis of their high grade, possessed a Nd isotopic signature that was in fact characteristic of another, usually low-grade unit, the Lesser Himalaya (LHS). This is probably due to the exposure of deep levels of the LHS by anomalously rapid Neogene exhumation. In detail, Lesser Himalayan rocks have ϵ_{Nd} values of -16 to -29, as opposed to -6 to -18 for the HHCS.

A context for the syntaxis

This study investigates a highly condensed section on the eastern margin of the syntaxis, where the influence of Neogene metamorphism on a mainly metasedimentary section becomes weaker eastwards. Model ages indicate that rock units with LHS and HHCS isotopic signatures are present, and in addition evidence for pre-Neogene and pre-Himalayan events is preserved. Sr isotopic data on the same section should confirm the presence of these units, and may also distinguish a further major unit: the Tethyan Sedimentary Series at the top of the nappe pile. Modelling of the Sr and Nd evolution of diverse granitoids in the syntaxis is in progress to distinguish their sources, particularly in relation to the host gneisses. These granitoids include a gneiss derived from an Ordovician granite (Foster et al 1999) at the basement/cover boundary within the HHCS section, and Ky-bearing leucogranites with a similar Nd signature to HHCS leucogranites in the central Himalaya.

References

- Foster, G. L., Kinney, P., Vance, D., Harris, N., Argles, T., and Whittington, A., (1999), in: *14th Himalaya-Tibet-Karakoram Workshop Abstract Volume* p.44-45
 Whittington, A. G., Harris, N. B. W., Ayres, M. W., and Foster, G. L., (1999), *Geology*, 27(7), 585-588.

Parental magmas for differentiated sills and large layered intrusions

A. A. ARISKIN

Vernadsky Institute, Moscow, Russia (ariskin@geokhi.ru)

Using the COMAGMAT crystallization model (Ariskin, 1999) low pressure phase equilibria calculations have been conducted for a set of rocks representing the Marginal Series and Lower Zones from the differentiated sills (Vavucan, (Vav) Talnakh, (Tal) Kamenistyi (Kam)) and large layered complexes, such as Skaergaard (Ska), Kiglapait (Kig), and Dovyren (Dov). It allowed us to define the range of initial temperatures and parental magma compositions intrinsic to the original crystal mush from which the most primitive rocks have been crystallized (table). In parallel, estimates of primary crystal-melt proportions for the intrusive magmas were obtained. These modal proportions indicate that the original magmatic suspensions may contain from few percents (Siberian traps) to 15-25% (Talnakh and Kiglapait), and even 50-70% of crystals (Dovyren and Partridge River intrusion). This is in general agreement with results of dynamic calculations simulating emplacement of a non-isothermal magma which show the primary crystallinity of intrusive magmas is strongly depend upon the extent of cooling during the injection process (Sharapov *et al.*, 1997). Coupled with the results of the phase equilibria reconstruction these evidences argue that almost instantaneous injection of super-heated melts into magma chambers is unrealistic. This means that an early crystal sedimentation and (probably) compaction of the crystal piles should be considered as an important initial stage of the formation of layered intrusions, whether the further fractionation is caused mostly by crystal settling out of suspension during viscous flow or from a dispersed state during slow growth in an advancing zone of crystallization.

Body	Vav	Tal	Kam	PRI	Ska	Dov	Kig
<i>h</i> , m	100	100	200	500	2500	3200	9000
<i>T</i> , °C	1195	1200	1170	1150	1165	1185	1230
SiO ₂	49.54	48.75	49.71	46.81	50.01	55.00	47.17
TiO ₂	1.19	1.30	1.39	1.15	1.68	0.74	1.08
Al ₂ O ₃	15.57	15.42	14.76	18.79	12.95	15.52	17.70
FeO	11.18	12.00	14.75	12.31	13.24	7.58	13.51
MnO	0.28	0.22	0.26	0.14	0.19	0.14	0.19
MgO	7.91	7.94	6.64	8.85	6.90	7.33	8.03
CaO	11.72	11.43	10.13	8.80	12.40	10.80	8.73
Na ₂ O	2.12	2.16	1.74	2.57	2.37	1.72	3.19
K ₂ O	0.36	0.65	0.41	0.46	0.26	1.08	0.28
P ₂ O ₅	0.13	0.14	0.21	0.12	0.15	0.08	0.12
<i>Primary crystals, wt.%</i>							
<i>Ol</i>	0.3	11.3	0.7	11.4	nd	46.5	4.8
<i>Pl</i>	1.8	2.7	41.3	56.6	nd	4.6	20.0

PRI – Partridge River intrusion.

References

- Ariskin A.A. (1999). *J. Volcan. Geotherm. Res.* **90**, 115-162.
 Sharapov V.N. *et al.* (1997). *Petrology* **5**, 10-22.

Sr isotope systematics in two glaciated crystalline catchments in the Swiss Alps

K. ARN¹, R. HOSEIN², K. B. FÖLLMI³, P. STEINMANN⁴, J. KRAMERS⁵, D. AUBERT⁶

¹⁻⁴Institut de Géologie, Université de Neuchâtel, Rue Emile-Argand 11, CH-2007 Neuchâtel, Switzerland

¹(kaspar.arn@unine.ch); ²(rachel.hosein@unine.ch)

³(karl.foellmi@unine.ch); ⁴(philipp.steinmann@unine.ch)

⁵Gruppe Isotopengeologie, Geologisches Institut, Universität Bern, Erlachstrasse 9a, CH-3012 Bern, Switzerland (kramers@geo.unibe.ch)

⁶EOST, ULP/CNRS, Centre de Géochimie de la Surface, UMR 7517, 1 rue Blessig, 67084 Strasbourg Cedex, France (daubert@illite.u-strasbg.fr)

The Sr isotope systematics are useful in the identification of the relative importance of different sources contributing to chemical weathering fluxes. We studied subglacial chemical weathering processes and the Sr isotope composition of runoff and particulate material in the two glaciated catchments of Oberaar (OA) and Rhone (RH) glacier (Swiss Alps). Both areas are contained within the crystalline rocks of the Aar Massif, and the lithologies are quite homogeneous and comparable, except for the presence of a zone of highly deformed variscide basement gneisses and schists in the Oberaar catchment.

We analysed meltwaters (RH ⁸⁷Sr/⁸⁶Sr = 0.7257 / OA 0.7155), suspended sediment (RH 0.7292 / OA 0.7134), precipitation (0.7104) and dust (0.7109), local bedrock (0.7101 – 0.7377), and subglacially precipitated calcite that is now exposed in front of the glaciers (RH 0.7182 / OA 0.7164).

RH meltwater ratio is smaller than RH suspended sediment (total digestions) which can be interpreted as a mixture of granodiorite (0.7101) and granite (0.7377). We explain this by the preferential weathering of calcite (disseminated or in veins), which has a relatively low ⁸⁷Sr/⁸⁶Sr ratio. An enrichment in Ca relative to Na in the meltwaters compared to suspended sediments is visible in both areas (OA > RH). In addition meltwaters could also be influenced by atmospheric input. The role of this will be assessed by mass balance calculations. The fact that OA meltwaters show an increased ratio compared to OA suspended sediment points to a minor atmospheric influence on our meltwaters: Increased OA meltwater ratios are better explained by the weathering of freshly ground biotite. The concentration of suspended sediment is higher for OA than for RH. OA suspended sediment contains more biotite due to the gneissic rocks within this catchment, what is also visible in the more elevated K flux.

The first order reaction in our catchments is weathering of calcite, but in addition, in the OA catchment biotite weathering exerts an other major influence on the meltwater ⁸⁷Sr/⁸⁶Sr ratio.

Geochemical comparison of Late Pliocene sapropels from the Vrica land section and ODP Sites 964 and 974

M. ARNABOLDI AND P.A. MEYERS

Department of Geological Sciences, The University of Michigan, Ann Arbor, MI, USA (marna@umich.edu)

The post-Miocene sedimentary record of the Mediterranean Sea records evidence of global climate variations characterized by a cyclicity of ~21kyr and induced by fluctuations in the orbital precessional cycle (e.g. Emeis et al., 1996). Sapropels are the expression of such climate changes. Their widespread occurrence allows reconstruction of the paleoceanographic processes involved in organic matter production and preservation, their variability through time and space, and evaluation of the relative importance of local factors. We studied two insolation cycles (i-cycle 178 and i-cycle 180) from the Vrica Section (Calabria, Italy) and ODP Sites 964 and 974. The Vrica Section is a paleomargin sequence characterized by high sedimentation rates at the edge of the Ionian Basin. In contrast, Sites 964 (middle of the Ionian Basin) and 974 (central Tyrrhenian Basin) represent open sea settings.

Methods and results

We analyzed a variety of geochemical proxies including contents of organic carbon and nitrogen, trace element compositions, C and N isotopic contents of bulk organic matter, and alkenone and *n*-alkane biomarker molecules. The Vrica section because of its high sedimentation rates allows observation of much finer details within the sedimentary sequence than either of the deep-sea Sites. At Vrica in fact we identified the presence of two interruptions and a pre-sapropel for i-cycle 178 and of two sub-units within i-cycle 180.

Conclusions

The comparison of the same sapropel sequences between multiple sites is particularly useful to understanding the major processes involved in sapropel deposition and the tuning operated by local factors. In particular, increased productivity at the sea surface, anoxia at the sea bottom, increased continental runoff and higher rates of nitrogen fixation (Struck et al., 2001) seem to be involved in sapropel deposition. The investigation of sites from different sub-basins is especially interesting in the evaluation of the synchronicity and strength of the global signal controlling sapropel events.

References

- Emeis K.-C., Robertson A.H.F., Richter C. et al., (Eds) (1996), *Proc. ODP. Init. Rep. 160*.
Struck U., Emeis K.C., Voß M., Krom M.D., Rau G.H., (2001), *Geochim. Cosmochim. Acta* **65**, 3249-3266.

High-K magmas from the French Massif Central: crust-mantle interaction during the Hercynian orogeny.

N. ARNAUD¹, A. AGRANIER^{1,2}, G. CHAZOT¹, C. PIN¹, J. L. POIDEVIN¹ AND J. BLICHERT-TOFT²

¹Magmas et Volcans, UMR6524 CNRS, 63000 Clermont-Fd, France (N.Arnaud@opgc.univ-bpclermont.fr)

²Ecole Normale Supérieure, 46 allée d'Italie, 69364 Lyon Cedex 7, France

The occurrence of highly potassic magmatism in active orogens is well documented. However, the nature of its source and the evolution of magmas during ascent is still debated and it remains to be shown whether such magmas can help trace mantle processes beneath orogenic areas. To better elucidate the interaction between high-K magmas and the crust, we analyzed so-far poorly characterized lamprophyres from mid to deep crustal levels of the eroded Hercynian orogen of the French Massif Central.

⁴⁰Ar/³⁹Ar dates obtained on biotite-rich minettes from the Cevennes located externally during orogeny and amphibole-rich spessartites from Auvergne located more centrally show that these high-K magmas were emplaced between 325 Ma and 310 Ma, during the late orogenic extensional phase and the late phase of granitic magmatism. Zoned biotites, calcic amphiboles and K-feldspars are the key minerals in these "calc-alkaline" lamprophyres. Although mechanical interaction between the lamprophyres and the surrounding granites is evident in the field, major and trace element compositions demonstrate that contamination was limited, and that biotite and/or amphibole were the only minerals to crystallize at depth. This suggests that the highly LREE-enriched lamprophyres represent early liquids from a metasomatized mantle source rich in either mica or amphibole and located at depths shallower than the garnet stability field, presumably the lithospheric mantle. Sr isotopes further indicate the mantle source was enriched during the Hercynian subduction, possibly with fluids with a sediment-like signature. Highly unradiogenic Nd and Hf isotope compositions require a time-integrated much older, perhaps Pan-african, reservoir.

These results show that in the present case (1) high-K volcanic rocks experienced only limited crustal interaction, suggesting rapid ascent through the crust, and thus may be representative of their mantle source; (2) shallow lithospheric mantle was melted during the late stages of orogeny; (3) the geochemistry is dominated by ancient and/or recent metasomatism. Because high-K orogenic magmatism appears chemically homogeneous in mountain belts through time, these conclusions may apply more generally thus throwing light on the key "mature" state of the orogenic process to be recognized in past orogens.

Komatiites, kimberlites and boninites

N. ARNDT

LGCA, Univ Joseph Fourier, Grenoble, France; arndt2ujf-grenoble.fr

When the mantle melts, it produces ultramafic magma instead of the more usual mafic magma, if (a) the site of melting is unusually deep, (b) the degree of melting is unusually high, or (c) the source is unusually refractory. For this to happen, the source must be unusually hot, or it must contain a high volatile content. Just as with basalts, different conditions of mantle melting produce a spectrum of ultramafic magma types.

Komatiites form by relatively high degrees of melting, at great depths, of an essentially anhydrous source. Barberton-type (or Al-depleted) komatiites are high-degree batch melts from a particularly hot source. The combination of high-degree melting and a garnet-subtraction geochemical signature requires that these melts formed at extreme depths (>300 km) from a source that may have been molten as it crossed the transition zone. Munro-type (Al-undepleted) komatiites lack the garnet-subtraction signature and are depleted in incompatible trace elements. They form through high-degrees of fractional melting from a slightly cooler source, at less extreme depths.

Kimberlites and meimechites are highly mafic to ultramafic alkaline magmas that form through low-degree melting, also at great depth, of sources that are enriched in incompatible elements and in CO₂ + H₂O. Their enormous trace-element concentrations and lithospheric or asthenospheric isotope compositions are not explained simply by partial melting. These magmas probably attain their final geochemical compositions during subsequent interaction with overlying asthenospheric or lithospheric mantle.

Boninites are highly mafic siliceous magmas produced by hydrous melting of metasomatised, originally depleted mantle wedge above a subduction zone.

Just like basalts, the different types of ultramafic magma, and their contrasting modes of formation, are readily distinguished using a combination of major and trace element characteristics.

Oxygenation of Proterozoic oceans: Insight from molybdenum isotopes

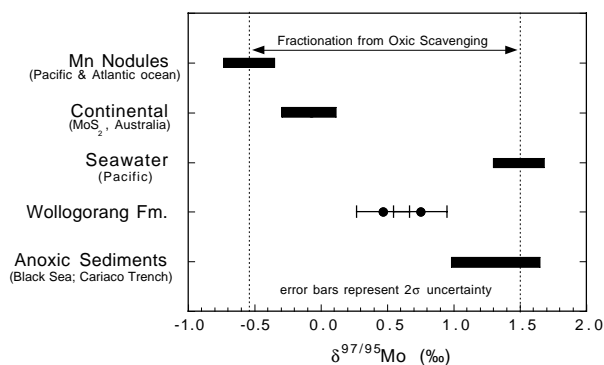
G. L. ARNOLD¹, A. D. ANBAR¹, J. BARLING¹

¹Department of Earth and Environmental Sciences, University of Rochester, Rochester, NY 14627 USA
(gail@earth.rochester.edu, anbar@earth.rochester.edu, barling@earth.rochester.edu)

The oceans in the mid-Proterozoic are classically thought of as fully oxygenated. However, S-isotope data suggest widespread sulfidic conditions (Canfield, 1998). Mo isotopes may provide insight to this debate.

Previously, we observed a systematic Mo isotope fractionation ($\delta^{97/95}\text{Mo}$) between recent oxic and anoxic sediments (Barling et al., 2001; Arnold et al., 2001; Fig. 1; data relative to laboratory standard). $\delta^{97/95}\text{Mo}$ of seawater and anoxic sediments are essentially the same, suggesting Mo isotope fractionation during removal to oxic sediments. Laboratory experiments support this suggestion (Barling and Anbar, 2001). Therefore, $\delta^{97/95}\text{Mo}_{\text{seawater}}$ may reflect the global balance between Mo removal to oxic and anoxic sediments and changes in this balance should be recorded as changes in $\delta^{97/95}\text{Mo}_{\text{anoxic}}$. If the proportion of seafloor under sulfidic waters were larger in the past, $\delta^{97/95}\text{Mo}_{\text{anoxic}}$ should shift toward lighter values. Assuming steady-state mass balance and data to date as representative, $\delta^{97/95}\text{Mo}_{\text{anoxic}} \sim 1.98 - 2.05 \times f_{\text{anoxic}}$.

Figure 1: $\delta^{97/95}\text{Mo}$ in geological materials



Preliminary investigation of ~ 1.73 Ga Mo-rich black shales from the Wollongorag Fm. (McArthur Basin, Australia) reveals unusually light $\delta^{97/95}\text{Mo}_{\text{anoxic}}$ (0.47 to 0.75 ‰). Mo in these sediments is primarily authigenic. These data suggest $f_{\text{anoxic}} = 0.60$ to 0.74 vs. ~ 0.22 today, consistent with more extensive sulfidic deposition in mid-Proterozoic oceans.

Arnold, G.L., Barling, J. and Anbar A.D. (2001), *Abstracts with Programs – GSA* **33**, 38.

Barling, J., Arnold, G.L. and Anbar, A.D. (2001), *EPSL* **193**, 447-457.

Barling, J. and Anbar, A.D. (2001), *Eos, Trans, AGU* **82**, 47.

Canfield, D.E. (1998), *Nature* **396**, 450-453.

Chemical environmental impact of geothermal resource utilization

STEFÁN ARNÓRSSON

Science Institute, University of Iceland, Dunhagi 3, 107
Reykjavík, Iceland stefanar@raunvis.hi.is

High-temperature geothermal resources are being increasingly exploited for power generation and low-temperature resources for direct use. In 1999 the installed capacity of geothermal power plants in the world was ~8000 MW (energy use = 49,000 GWh). The corresponding numbers for direct use were 11,000 MW and 53,000 GWh. The environmental impact of geothermal power plants includes chemical pollution from gaseous components in steam and dissolved solids in water, scenery spoliation, land erosion, noise and sometimes subsidence. In the last 20 years, or so, the environmental impact has been reduced by injecting into wells waste water and condensate. At some geothermal power plants, the H₂S in the steam is removed before disposal to reduce atmospheric pollution. Generally cooling towers have been used for steam condensation, the purpose of condensation being to improve the efficiency of steam exploitation. A notable exception is the Nesjavellir power plant, Iceland where the steam is condensed in heat exchangers. With this layout, and the injection of waste water and condensate into wells, surface installations are effectively a closed loop between production and injection wells, thus minimizing the environmental impact of the utilization of the geothermal resource. The environmental impact of direct use of low-temperature geothermal resources is much less than that of high-temperature ones and generally very insignificant with respect to chemical pollution.

Geothermal fluids show very wide ranges in chemical composition ranging from <1000 ppm dissolved solids in systems hosted by basaltic rocks to >30% in systems in sedimentary rocks containing evaporites. Correspondingly large variations occur in the concentrations of air- and water-borne poisons in these fluids. Water-borne poisons include As, B, Hg, H₂S, NH₃, sometimes Al and various heavy metals in addition to high salt content. Air-borne poisons include As, Hg and H₂S in addition to the greenhouse gases, CH₄ and CO₂. The concentrations of environmentally harmful chemical constituents in geo-thermal fluids are related to their geological setting, the rock types that host them and aquifer temperature.

The activities of reactive components in >100°C geothermal fluids are controlled by temperature dependent secondary mineral-solution equilibria. By contrast, the concentrations of conservative components (e.g. Cl, B, As) are determined by their supply to the geothermal fluid which may come from the rock with which the fluid has reacted, the magma heat source or the parent fluid. Because of this, geothermal fluid compositions are to some extent predictable, including poisons compounds, in terms of aquifer temperature, salinity and geological environment.

Carbon Cycling in a Continental Margin Sediment: Contrasts Between Organic Matter Characteristics and Remineralization Rates and Pathways

C. ARNOSTI¹ AND M. HOLMER²

¹Marine Sciences, Univ. North Carolina, Chapel Hill NC
27599-3300 USA (arnosti@email.unc.edu)

²Inst. of Biology, Univ. Southern Denmark, Campusvej 55
Odense 5230 Denmark (holmer@biology.sdu.dk)

In Skagerrak, chemical characterization suggested that sedimentary organic matter was similar at 3 stations, with high C/N, just 12% of TOC characterizable at a molecular level, and little downcore variation in total organic carbon, total hydrolysable amino acids, or total hydrolysable carbohydrates. All of these parameters are characteristic of 'low quality' and not particularly reactive organic matter. Measurements of the terminal steps in the carbon remineralization pathway, however, presented a different picture. Net carbon oxidation rates at all three stations were relatively high, and differences in terminal remineralization processes (sulfate, iron, and manganese reduction) implied differences among the microbial communities active in these sediments. Measurements of enzymatic hydrolysis rates also demonstrated depth-, substrate, and site-related differences in potential enzyme activities. A comparison of dissolved organic carbon (DOC) inventories with enzymatic hydrolysis and terminal remineralization rates demonstrated that turnover of at least a portion of the DOC pool must be rapid, hence conversion of POC to DOC must also be sufficiently fast to maintain the DOC pool. Standard methods of bulk chemical characterization of sedimentary organic matter are clearly insufficient in this case to reveal variabilities in organic matter reactivity that are important at a microbial scale.

Search for an extraterrestrial impact record in Isua sediments

G. ARRHENIUS¹, A. LEPLAND², AND F. ASARO³

¹SIO-UCSD, La Jolla CA 92093 0220, (arrhenius@ucsd.edu)

²NGU, Trondheim NO 7491 (aivo.lepland@ngu.no)

³LBNL, Berkeley CA 94720, (F_Asaro@lbl.gov)

The cratering record of impacts on the Moon has led to the common belief that the Earth must have experienced an even stronger, gravitationally enhanced late bombardment, culminating around 3.8 Ga and decaying during the next 0.3 Ga.. However, no evidence for such violent impacts or accompanying flux of extraterrestrial dust has been found in the fragmentary terrestrial rock record.

The sequences of sedimentary banded iron formations (BIFs) in the ca. 3.8 Ga Isua supracrustal belt contain heavily disturbed, coarse-grained sediment packages that could possibly be impact related. In order to test this possibility we have determined the content of iridium with precisions of measurement between 2 and 8 parts per trillion (ppt) in a profile across a disturbed bed and adjacent undisturbed BIF.

The measured Ir concentrations are well below typical crustal values and range from less than precisions to 12 ppt.. The Ir concentrations in the disturbed bed do not show meaningful trends or a systematic contrast between this bed and adjacent, finely laminated sediment strata.

The exceptionally low Ir abundances do not provide support for the concept of a high flux rate of extraterrestrial material during accumulation of Isua sediments, placing our study in the group of several recent unsuccessful efforts to find such an enhancement in the oldest terrestrial rock record. Comments in the literature on the missing dust- and impact features make inconsistent reference to the lunar record by assuming that the late lunar bombardment ceased 3.8 Ga ago, ignoring the fact that it continued at a decreasing rate to about 3.5 Ga. The terrestrial record has recently been extended back in time to 4.4 Ga with data indicating the presence of a hydrosphere at several points in the time interval 3.8 – 4.4 Ga. These results can be taken to suggest cooling of the Earth between impact events, variably estimated to partly or entirely vaporize the hydrosphere or to convert the planetary surface to a magma ocean. With increasing density of observations in the earliest planetary record, the need is growing for an alternate explanation of the late lunar bombardment.

Variations in carbonate mineral dissolution rates: experimental uncertainty or fundamental property?

R. S. ARVIDSON AND A. LUTTGE

Rice University, Dept. of Earth Science, 6100 Main Street, Houston TX 7005 (rsa4046@ruf.rice.edu)

A review of calcite dissolution rates far from equilibrium reveals that despite high internal consistency among rates reported by a given laboratory, there are significant discrepancies in absolute values. This variation has been recognised before (e.g., Dove and Platt 1996), and has been assumed to reflect differences in reactive surface area. In addition, both atomic force microscopy and vertical scanning interferometry (VSI) rate data for calcite, as well as VSI data for dolomite, are significantly lower than surface area-normalised-rates derived from powdered materials or single crystal rotating disk experiments.

Here, we test the hypothesis that the variation in reported rates reflects the distribution of different reaction mechanisms. VSI data suggest that bulk rates reflect the sum of related but distinct processes: rapid dissolution at deep etch pits

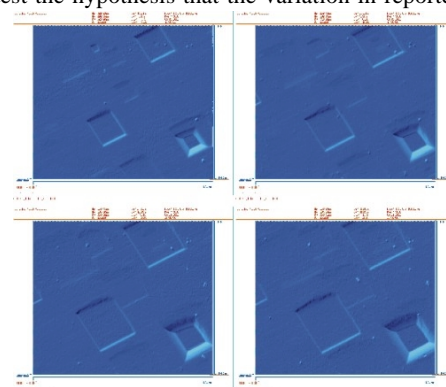


Figure 1: Etch pits at 30 minute time steps (VSI data). Rate = $10^{-11.6}$ mols/cm²/s, pH 8.8, P_{CO2} 10^{-3.4}, 25°C.

(Figure 1; cf. AFM data of MacInnis and Brantley 1993, Liang et al. 1996), the development of shallow, ephemeral etch pits, and the relatively slow (in the case of calcite) rate associated with global step movement. In addition, grain boundaries in powders may play a special role in terms of step generation. In our single crystal experiments, large variations in the distribution of deep etch pits at dislocations imply similar variations in the corresponding bulk rate for powders, and thus the expectation of a unique bulk rate may not be warranted. The only rate that may be considered constant for a given set of conditions is that of global step movements.

References

- Dove P.M. and Platt F.M. (1996) *Chem. Geol.* **127**, 331-338.
 Liang Y., Baer D. R., McCoy J. M., Amonette J.E., and LaFemina J. P. (1996) *Geochim. Cosmochim. Acta* **60**, 4883-4887.
 MacInnis I.N. and Brantley S.L. (1993) *Geochim. Cosmochim. Acta* **56**, 1113-1126.

Hf-Nd isotopic variations of authigenic and silicate components in north Pacific sediments

Y. ASAHARA¹, D.-C. LEE², M. FRANK², T. VAN DE FLIERDT², A. N. HALLIDAY² AND A. NISHIMURA³

¹ Dept. of Earth and Planetary Sciences, Nagoya University, Chikusa, Nagoya 464-8602, Japan (asahara@eps.nagoya-u.ac.jp)

² Dept. of Earth Sciences, ETH Zurich, Switzerland

³ Geol. Surv. Japan, AIST, Tsukuba 305-8567, Japan

Recent studies of hydrogeneous Fe-Mn crusts have shown that Hf and Nd isotope time series in seawater are decoupled despite the similar geochemistry of these elements in the mantle and similar residence times in seawater. It is considered that the decoupling is either caused by a slight difference of oceanic residence time of Hf and Nd or a different behavior of these elements during weathering of continental crust. We determined Hf and Nd isotope compositions of both silicate and authigenic fractions in north Pacific surface sediments in order to understand the behavior of Hf and Nd in seawater at the present time. Weathering products in the Asian continent (loess, river deposit and desert sand) were also examined. After carbonates in these samples had been dissolved in weak hydrochloric acid (0.25M), Fe-Mn components were leached with oxalic acid (0.1M). The residues were defined as silicate components.

For the silicate fractions, ϵ_{Nd} of deep sea sediment in the north central Pacific (-10 to -7) and ϵ_{Hf} and ϵ_{Nd} of continental shelf sediments in the Yellow Sea and the East China Sea (-24 to -7 and -14 to -10, respectively) are similar to those of the Asian continental material (ACM) ($\epsilon_{Hf} = -17$ to -14 , $\epsilon_{Nd} = -12$ to -10). ϵ_{Hf} in the north central Pacific (-4 to 0) is obviously higher than that of ACM. ϵ_{Hf} in grain size fractions of ACM shows large variations from -16 to -4 and that in $<2 \mu\text{m}$ fraction of the Asian loess is -4. This confirms previous evidence that the fine particles of the weathering products in the Asian continent are transported into the north central Pacific by wind and dominate the pelagic sediments.

The regional variations in Hf and Nd isotopic compositions in the oxalic acid leachates of deep sea sediments are consistent with published data for Fe-Mn crusts. This suggests that Hf and Nd in the leachates of these sediments have seawater origin.

The Nd isotopic composition of the oxalic acid leachate of ACM is similar to that in silicate fraction of ACM ($\epsilon_{Nd} = -12$ to -10), while the Hf isotope composition of the leachate ($\epsilon_{Hf} = -1$ to $+11$) is significantly higher than that of the silicate fraction. This suggests the different behavior of these elements during weathering process. Furthermore, the Hf isotope composition of the ACM leachate is quite similar to that in seawater. The easily dissolved fraction in eolian dust from the Asian continent is a possible significant source of Hf to seawater.

Was ²⁶Al a chronometer or heat source in the early solar system?

R. D. ASH¹, S. S. RUSSELL², M. GOUNELLE², E. D. YOUNG¹ AND N. C. BELSHAW³

¹ Department of Earth and Space Sciences, 595 Charles E. Young Drive East, Geology Building, Los Angeles, CA 90095-1567, USA (e-mail rash@ess.ucla.edu),

² Department of Mineralogy, The Natural History Museum, Cromwell Road London, SW7 5BD, UK..

³ Dept. Earth Sciences, University of Oxford, Oxford OX1 3PR, UK

Chondritic meteorites are often considered to be representative of materials which accreted to form planets. ²⁶Al (half life 730000yrs) is commonly used as a high resolution chronometer for comparing events early in the solar system, as recorded by these chondrites; it is also appealed to as a heat source for planetesimal thermal processing. It is also considered a viable heat source for the early melting of terrestrial planets. Some of these characteristics appear mutually exclusive, particularly when considered in the light of chondrite evolutionary pathways.

Calcium-Aluminium-rich Inclusions (CAIs) are probably the earliest extant solids formed in the solar system and contain the highest initial ²⁶Al abundances. Studying the systematics of ²⁶Al within CAIs should help us understand the evolution of ²⁶Al in other chondritic materials and, ultimately, its role in the early solar system.

We have used laser ablation MC-ICP-MS (ArF excimer UV laser coupled to a Nu Instruments ICP-MS) to measure low Al/Mg minerals in a Type B Leoville (CV3) CAI. The CAI exhibits typical igneous texture with a melilite-spinel-fassaite-anorthite core surrounded by a melilite mantle containing minor spinel. For ion microprobe analysis only anorthite would be suitable for high precision Al-Mg chronology due to its high Al/Mg. By the application of high precision ICPMS we can determine Al-Mg ages on spinel, fassaite and melilite (though not anorthite due to low Mg abundances).

Results demonstrate that the outermost part of this inclusion underwent isotopic exchange and re-equilibration, probably in a nebula resetting after the complete decay of ²⁶Al. In the classical interpretation of variations in ²⁶Al/Al, CAI evolution and the vision of chondrites as planetary precursors would imply that ²⁶Al had entirely decomposed prior to the final accretion of chondritic parent bodies hence would not be available for the heating of planetesimals and planets.

These results suggest that the early evolution of chondritic materials occurring sequentially as: CAI formation, chondrule formation, accretion, lithification, planetesimal melting did not occur prior to the complete decay of ²⁶Al, there was still nebula processing after the complete decay.

Geochemical evidence for multistage melt percolation in mantle keel beneath Wyoming craton.

ASHCHEPKOV I.V.¹, VLADYKIN N.V.², MITCHELL R.H.³,
COOPERSMITH H.⁴, SAPRYKIN A.I.¹, GARANIN.V.G.¹
ANOSHIN G.N.¹, KHMELNIKOVA O.S.¹,

¹UIIGM SDRAS, Novosibirsk, Russia, (garnet@uiggm.nsc.ru)

²IGC SDRAS, Irkutsk, Russia, (vlad@igc.irk.ru)

³Lakehead University, Canada, (rmitchel@gale.lakeheadu.ca)

⁴Great Western Diamond Co., USA, (diamonds@verinet.com)

Results

Garnet and clinopyroxenes from concentrate KL-1 pipe Front Range kimberlite group Colorado display several trends (3) varying in Ti and Na contents. Cr-Ca trends in lherzolite fields (Sobolev, 1977) is less than for Iron Mt kimberlite (Hausel, 1998). In L-Ti groups Ga and Cpx both have strong U peaks correlating with La/Yb_n ratio for Cpx and parental melts. Some Cpx and other minerals show small Eu minima. Spinels reveal joint Al-Ti enrichment. Ilmenites display several descending Ti-Al-Mg and Mn (up to 12%) trends. The most Cr-rich garnets (to 12%) and ilmenites (to 8% Cr₂O₃) were found in harzburgites. Clinopyroxene thermobarometry (Nimis, Taylor, 2000; Ashchepkov, 2002) suggest heating for deformed L-Ti intergrowths of Cpx and Ga comparing with the separate Cpx grains.

Discussion

Several pulses of melt percolation suggest long history for mantle evolution with the participation of subduction related eclogites and possibly sea floor (Mn) sediments in melt generation region at the last stages. Ti-low pyroxenes were associated with deformations caused by deep subduction.

Conclusion

Mantle column beneath KL-kimberlite pipe was modified by Ti rich plum- related and then by melts contaminated in subducted material. Grants RBRF 05-99-65688 05-00-65288.

References

- Ashchepkov I.V. (2002). *Trans RAS (ESS)*, 301, 78-82
Hausel, W.D. (1998). *WSGS Report 53*, 93 p.
Nimis P., Taylor W., 2000. *CMP*, 139, 541-554
Sobolev, N.V. 1974. *AGU, Washington, DC*, 279 pp.

Melt migration vs. isentropic decompression melting, more or less

PAUL D. ASIMOW

Division of Geological and Planetary Sciences 170-25,
California Institute of Technology, Pasadena, CA 91125
USA; asimow@gps.caltech.edu

Decompression melting of the asthenospheric mantle is routinely modelled as an isentropic process, but as thermodynamic models evolve to the point where this constraint can be rigorously (and perhaps accurately) imposed, it becomes important to test the quality of this assumption. In particular, as McKenzie (1984) recognised, when melt migration occurs the upwelling is neither adiabatic nor reversible due to advection of heat by the melt and gravitational dissipation. McKenzie estimated that these effects were negligible relative to the rather large uncertainties in his melting parameters, but concluded that *melt migration leads to excess melting* above that generated in the isentropic case, by at most 60%. However, relative movement of melt and solids has another first-order effect — the possibility of introducing chemical disequilibrium, or something akin to fractional melting. It is well known that fractional melting processes are less productive in general than equilibrium melting, so this raises the possibility that *melt migration leads to substantially less melting* and crustal production than the isentropic equilibrium case. In order to settle which of these effects is dominant and to bound the magnitude of both effects, I construct an energy equation similar to McKenzie's that allows for chemical and thermal disequilibrium between migrating melts and residues and perform a series of one-dimensional MELTS calculations that show the net melt production of various cases.

For normal oceanic potential temperatures (sufficient to generate 3-9 km of crust), *the extra crustal thickness generated by gravitational dissipation is no more than ~100 m*. This number is much smaller than McKenzie's estimate for two reasons: the effective limitation of melt production by clinopyroxene exhaustion and low melt productivity near the solidus (Asimow et al., 1997). In the absence of steep melting or freezing fronts dissipation due to viscous solid compaction is negligible, but I have not treated dissipation due to shear of the matrix. The possibility that migrating melts may escape hotter than the melting adiabat is in fact a way to *reduce* crust production by ~100 m, not a source of excess melt relative to the isentropic case. Most importantly, *disequilibrium flow decreases crustal production by 1-2 km relative to batch melting*. In short, if melt migration leads to chemical isolation it strongly suppresses melting but the isentropic model remains an excellent approximation of equilibrium flow and the incrementally isentropic model an excellent approximation of disequilibrium flow.

Asimow P.D., M.M. Hirschmann & E.M. Stolper (1997) *Phil. Trans. Roy. Soc.* **A355**:255-281.

McKenzie D. (1984) *J. Petrol.* **25**:713-765.

Petrographical and Geochemical Features of the Mafic Microgranular Enclaves in the Torul (Gumushane) and Sarihan (Bayburt) Granitoids, NE Turkey

ZAFER ASLAN¹, ABDULLAH KAYGUSUZ¹, CUNEYT SEN² AND MEHMET ARSLAN²

¹ KTU, GMF, Department of Geological Engineering, Gumushane/TURKEY (aslan@ktu.edu.tr)

² KTU, MMF, Department of Geological Engineering, Trabzon/TURKEY

In this study, we presented petrographical and geochemical data of mafic granular enclaves (MME) of two fairly well studied Upper Cretaceous granitic batholiths in the Gumushane and Bayburt region of the eastern Pontides. The Sarihan Granitoid has simple petrography with quartz-monzodiorite, granodiorite and quartzdiorite, which contains dioritic and quartz dioritic MMEs. MMEs have very sharp contacts with host rocks, and are oval shaped with 3-5 cm in diameters. There is biotite enrichment and some large K-feldspar growths around contact of enclaves. The composite zoned Torul Granitoid is made up from quartz diorite, granodiorite, monzogranite, quartz monzodiorite, monzodiorite and siyenogranite. Along the zones, each member contains more basic members enclaves for example dioritic enclaves are seen in quartzdiorite and monzogranites includes granodioritic and quartz monzodioritic enclaves.

MMEs of the Sarihan and Torul Granitoids show similar geochemical characteristics with host rocks. While MMEs of Sarihan Granitoid contain 58.0-60.1 wt% SiO₂, 15.4-16.1 Al₂O₃, 4.1-6.2 Na₂O, 1.2-3.1 K₂O, the MMEs of Torul samples yield 52.4-55.9 % SiO₂, 16.4-19.0 Al₂O₃, 3.2-4.1 Na₂O, 1.2-2.5 K₂O. All of the Sarihan and Torul Granitoid samples are subalkalic and calc-alkaline. All MMEs in both plutons have the ratio of A/CNK>1 and the MMEs of Sarihan are somewhat more aluminous in character than the MMEs of Torul. They also show characteristics of CAFEM_C trend and volcanic arc granitoid. Rb varies in both suites from ~25-100 ppm. Zr is between 55-180 ppm in both granitoids. Similar LIL enrichment with host rocks is seen ORG normalized trace element compositions of the MMEs of Sarihan and Torul Granitoids. Chondrite normalized rare patterns of Torul Granitoids are smooth and moderately enriched in the light REE; (La/Yb)_N ranges from 3.0-8.5 and noticeable Eu anomaly is present.

Although general petrographical characteristics of MMEs of the Sarihan Granitoid and Torul Granitoid, MME are more basic and fine-grained compared to host rocks. The mineralogical features of MMEs indicate magmatic origin. Oval but not elongated shapes of MMEs suggest little internal flow within parental magma during emplacement. Although all MMEs show chemical and mineralogical related with the host rocks as a differentiation processes, some mineralogical features of MMEs of Sarihan may keep some evidences of magma mixing processes during Newtonian and visco-plastic stage.

Timescale of melt differentiation from ²³¹Pa-²²⁶Ra data

Y. ASMEROM¹, S. MUKASA², H. CHENG³, V. POLYAK¹
R.L. EDWARDS³

¹Dept. of Earth & Planetary Sciences, University of New Mexico, Albuquerque, NM 87131; asmerom@unm.edu
²Dept. of Geological Sciences, University of Michigan, Ann Arbor, MI 48109

³Department of Geology and Geophysics, University of Minnesota, Minneapolis, MN 55455

Constraints on time-scale of melting, melt transport and melt differentiation are critical to our understanding of mantle melting processes. U-series isotopes have the potential to provide quantitative constraints on timing and time-scale of melting and melt differentiation, while at the same time giving extent of chemical fractionation. ²³¹Pa and ²²⁶Ra, with half-lives of 32ky and 1.6ky respectively, present the greatest opportunity. Results from the Luzon Arc, the Philippine Archipelago, suggest a melt differentiation timescale of about 27 ky. Moreover, the ²³¹Pa and ²²⁶Ra data indicate two contrasting time-scales, with the ²²⁶Ra chronometer giving much shorter apparent timescale.

Historical eruption in Taal (Luzon Arc) range from undifferentiated lavas (basalts with <52 wt.% SiO₂) to more differentiated ones (dacites with up to 68 wt. % SiO₂). A basalt sample has the highest (²³¹Pa/²³⁵U) and (²²⁶Ra/²³⁰Th) (activity ratios), both at 1.5. (²³¹Pa/²³⁵U) is strongly positively correlated with MgO (an index of differentiation), with an R² value of 0.995. If one assumes that lavas originated from a parent magma with similar initial (²³¹Pa/²³⁵U) (not necessarily the same parent magma), then it is possible to calculate differentiation model ages for the various degrees of differentiation relative to an assumed parent initial or relative to the least-differentiated erupted lava. Using the later approach, we calculate differentiation from our least-evolved sample to the most evolved one to be around 27 ky. The (²³⁰Th/²³⁸U) data, although with much less spread (given the much longer half-life of ²³⁰Th and small initial deviation from secular equilibrium), support the (²³¹Pa/²³⁵U) chronology. Alternatively, the trend may reflect mixing between mafic magma and old felsic crust. However this is unlikely as the lavas have a very restricted range of long-lived isotopic values. For example, the ⁸⁷Sr/⁸⁶Sr ratios of the whole suite range from 0.70452 to 0.70459, while the ¹⁴³Nd/¹⁴⁴Nd ratios (normalized to ¹⁴⁶Nd/¹⁴⁴Nd = 0.7219) vary between 0.51281 and 0.51283. A timescales of magma differentiation in the range of 27 ky, inferred from (²³¹Pa/²³⁵U) data, is considerably longer than that inferred from our (²²⁶Ra/²³⁰Th) data or estimates by other workers also based on ²²⁶Ra data. The ²³¹Pa timescale more likely to represents the full differentiation history, while the ²²⁶Ra timescale may represent the last phase of differentiation, analogous to the notion of different closure timescales in long-lived radiogenic isotopes.

Carbon and water in Pitcairn and Society hotspots, French Polynesia

CYRIL AUBAUD¹, FRANÇOISE PINEAU¹, MARC JAVOY¹, ROGER HÉKINIAN² AND JEAN-LOUIS CHEMINÉE³

¹ Lab. de Géoch. des Iso. Stables. – I.P.G. Paris – FRANCE
(aubaud@ipgp.jussieu.fr)

² IFREMER, Centre de Brest, Plouzané – FRANCE

³ Obs. Volc. – I. P. G. Paris – FRANCE

It is well established that OIB have different Sr-Nd-Pb isotopic characteristics than MORB. However, carbon and hydrogen isotopic signatures of their sources remain largely unknown.

We analysed 53 volcanic glasses from seamounts in Pitcairn and Society hotspot areas (French-German cruise POLYNAUT) for CO₂, H₂O, δ¹³C and δD by crushing/step-heating/manometry/mass spectrometry techniques for volatiles in vesicles and dissolved in the glass.

Vesicularities of basalts vary from 1.6 to 50 vol%. Concentrations of carbon in vesicles vary by three orders of magnitude (from 0.8 to 870 ppm). Range of δ¹³C of CO₂ in vesicles (from -4.8 to -15.7 ‰) is the largest ever measured for oceanic glasses and extends to very low values. Range of water concentration (from 0 to 1600 ppm) and δD (-28 to -98 ‰) in vesicles is also wide. Concentrations (27 to 35 ppm) and δ¹³C (-10.8 to -15.2‰) of dissolved carbon in the glass are low whereas concentrations (6400 to 9900 ppm) and δD (-50 to -60 ‰) of dissolved water are high in comparison with MORB. Difference between δ¹³C of CO₂ in vesicles and δ¹³C of dissolved carbon is high (from +3.3 to +6.2‰).

The strong correlation between carbon concentration and δ¹³C of CO₂ in vesicles is the result of open system degassing. This is the first time that such a process is shown so evidently in vesicles of oceanic glasses. It confirms that a strong carbon isotopic fractionation (Δ¹³C ≥ +3.5‰) occurs during degassing and leads to very low δ¹³C values which are not the result of contamination or mixing with, for example, a low δ¹³C recycled component. Therefore, all concentration and isotope variations are the result of degassing. Two-stage degassing modelling suggests that distillation is a late stage (edifice and crust) process and is preceded by a large closed system degassing.

Reconstruction of concentrations in magmas before degassing suggests high concentrations of carbon and water (1 wt% for both). It supports the idea that Pitcairn and Society hotspots are enriched in volatiles (both H₂O and CO₂). There is no evidence for carbon isotopic heterogeneity (sources at -4±1‰ similar to sub-oceanic and sub-continental mantles as sampled by MORB and diamonds). However, the reconstructed δD in Pitcairn source is -50‰, significantly higher than depleted MORB (-80‰). Hypotheses of involvement of primordial and/or recycled material to the EM I Pitcairn source will be discussed at the conference.

Origin and migration of atmospheric REE in soils and surface waters

D. AUBERT¹, P. STILLE², A. PROBST³

¹ Ecole et Observatoire des Sciences de la Terre/Centre de Géochimie de la Surface, Strasbourg, France
(daubert@illite.u-strasbg.fr)

² Ecole et Observatoire des Sciences de la Terre/Centre de Géochimie de la Surface, Strasbourg, France
(pstille@illite.u-strasbg.fr)

³ Laboratoire des Mécanismes de Transferts en Géologie, Toulouse, France (aprost@cict.fr)

The aim of this work was to elucidate the origin and the migration of REE in soils and surface waters of a small forested catchment located in the Vosges mountains (France). Particularly, we try to estimate the respective contributions of atmospheric REE inputs and REE released during the weathering in the soils and surface waters using Sr and Nd isotopes.

Rainwater samples are strongly LREE depleted. Compared to urban precipitation collected in Strasbourg, the Vosges rainwater sample is significantly less REE enriched. However, both samples show more or less similar shapes of their REE distribution patterns.

The REE distributions in the spring- and streamwaters from the Vosges catchment are very different from those of the atmospheric solutions. Their Sr and Nd isotopic data suggest that most of the Sr and Nd originate from apatite leaching or dissolution. Soil solutions and soil leachates from the upper soil horizons have REE distribution patterns close to those of lichens and throughfall. Throughfall is slightly more enriched especially in light REE than filtered rainwater probably due to leaching of atmospheric particles deposited on the foliage and also to leaf excretion.

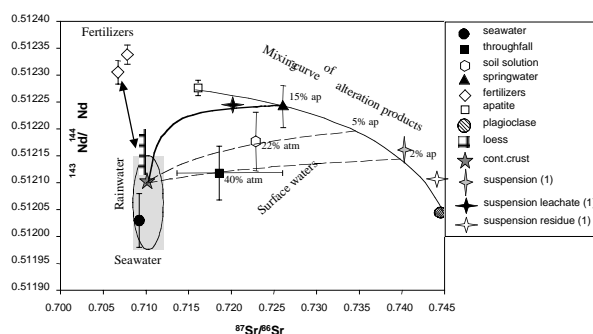


Figure 1: Sr and Nd isotopic compositions of the different samples collected in the Strengbach catchment (Vosges Mountains, France)

Data suggest (Fig. 1) that Sr and Nd isotopes of the soil solutions in the upper soil horizons originate from two different sources: 1. An atmospheric source with fertilizer, dust and seawater components and 2. A source mainly determined by mineral dissolution in the soil. The atmospheric contributions of Sr and Nd to throughfall and soil solution are of 20%-70% and 20%, respectively.

Carbon and oxygen isotopic composition of brachiopod shell calcite: physiological and environmental controls

ANNE-CÉCILE AUCLAIR¹, MICHAEL JOACHIMSKI² AND CHRISTOPHE LECUYER¹

¹Lab. PEPS, bat 402, Université Claude Bernard Lyon 1, 27-43 bd du 11 nov. 1918, 69622 Villeurbanne, FRANCE.

(Anne-Cecile.Auclair@univ-lyon1.fr, Christophe.Lecuyer@univ-lyon1.fr)

²Institut für Geologie und Mineralogie der Universität Erlangen-Nürnberg, Schlossgarten 5, 91054 Erlangen, GERMANY. (joachimski@geol.uni-erlangen.de)

This contribution aims to unravel the environmental and physiological controls on the stable isotope composition of modern brachiopod shell calcite. Based on SEM studies of the shells, a three dimensional high resolution sampling (< 500 μm) was performed on various modern brachiopod species (*Terebratalia transversa*; *Neothyris*; *Fallax*) in order to investigate carbon and oxygen isotope variations.

The primary shell layer as well as the outer part of the secondary shell layer of the thick shells of *Terebratalia* and *Neothyris* display large and variable negative offsets in comparison to calculated equilibrium values (as high as 6‰ for $\delta^{18}\text{O}$ and 7‰ for $\delta^{13}\text{C}$ in *Terebratalia*, and 3‰ for $\delta^{18}\text{O}$ and 5‰ for $\delta^{13}\text{C}$ in *Neothyris*). The positive correlation between $\delta^{18}\text{O}$ and $\delta^{13}\text{C}$ values ($r^2 > 0.8$) suggests that the stable isotope composition of these shell domains are mainly controlled by kinetic isotope fractionation effects. The isotopic offsets from equilibrium values preclude to calculate oceanic temperatures. However, ontogenetic variations in $\delta^{18}\text{O}$ and $\delta^{13}\text{C}$ ($\delta^{18}\text{O} \approx 4\text{‰}$ and $\delta^{13}\text{C} \approx 5\text{‰}$ in *Terebratalia*; $\delta^{18}\text{O} \approx 2\text{‰}$ and $\delta^{13}\text{C} \approx 3\text{‰}$ in *Neothyris*) observed in the outer part of the secondary layer can be used to plot growth curves for these specimen. Further analyses show increasing stable isotope compositions from the outer towards the inner part of the secondary layer, where the values reach expected equilibrium. This suggests a deceleration of calcite secretion during shell thickening.

In comparison to *Terebratalia* and *Neothyris*, the very thin shell of *Fallax* displays carbon and oxygen isotope values close to equilibrium with seawater, and kinetic effects seem to be of minor importance.

In conclusion, we suggest that isotopic studies of modern or fossil brachiopod shells should be combined with SEM observations of shell microstructure, which provide valuable information with respect to growth rate and processes during shell growth. A 3D sampling procedure should be used in order to isolate the shell parts less affected by physiological effects, *i.e.* more reliable for environmental reconstructions.

Magmatic anhydrite in the Cu-porphyry-related magma at Santa Rita, New Mexico (U.S.A.)

A. AUDÉTAT¹, T. PETTKE², D. DOLEJS³, R. BODNAR⁴

¹Institute of Mineralogy, University Tübingen, Germany (andreas.audetat@uni-tuebingen.de)

²Institute of Isotope Geochemistry, ETH Zürich, Switzerland (thomas.pettke@erdw.ethz.ch)

³Dept. of Earth and Planetary Sciences, McGill University, Montreal, Canada (dolejs@eps.mcgill.ca)

⁴Dept. of Geological Sciences, Virginia Tech, Virginia, U.S.A. (bubbles@vt.edu)

The formation of sulfides and immiscible sulfide melts is drawing increasing attention in research related to Cu-porphyry deposits (e.g., Halter et al., this session). It has been suggested that such sulfide phases act as temporary "storage medium" for chalcophile metals like Cu and Au (thus preventing them to be incorporated at trace-levels in other minerals), and supply the metals to the mineralizing fluids during a later stage of sulfide oxidation. Recent reports on the abundance and chemical composition of sulfide phases in natural systems seem to support this model of metal enrichment^{1,2}.

Here we present petrographic and analytical evidence for the occurrence of anhydrite in the ore-forming magma at Santa Rita, New Mexico. A pre-mineralization quartz-monzodiorite dike related to the mineralized stock contains anhydrite inclusions within apatite microphenocrysts. The rock also contains 1-2 vol-% cavities that, on the basis of petrographic relationships, can clearly be identified as former anhydrite phenocrysts. The stable assemblage of quartz + magnetite + sphene indicates a magmatic oxygen fugacity of $\geq (\text{NNO}^{+2})$, consistent with a lack of primary sulfides (or oxidized remains thereof)³. A similar situation has been reported from the mineralized Yerington Batholith, where the presence of magmatic anhydrite was inferred from calculated oxygen and sulfur fugacities⁴.

These examples demonstrate that significant Cu-porphyry mineralization can be generated *without* the formation of magmatic sulfides or immiscible sulfide melts. Magmatic sulfide exsolution thus appears not to be a prerequisite for the formation of economic Cu-porphyry deposits. Common to all magmas related to porphyry-type mineralization, however, seems to be a high sulfur-content (independent of the oxidation state), suggesting that this is one of the essential conditions for the genesis of such deposits.

¹Keith J.D. et al. (1997), *J. of Petrology* **38**, 1679-1690

²Halter W. et al. (2002), *Science* (in press)

³Carroll M. and Rutherford M. J. (1988), *Am. Mineral.* **73**, 845-849

⁴Streck M.J. and Dilles J.H. (1998), *Geology* **26**, 523-526

Sedimentary sources revealed by Nd isotopes: the Late Palaeozoic of southern Andean Patagonia

CARITA AUGUSTSSON^{1,2} AND HEINRICH BAHLBURG¹

¹Geologisch-Paläontologisches Institut, Westfälische Wilhelm-Universität, Corrensstrasse 24, 481 49 Münster, Germany (augustss@uni-muenster.de, bahlbur@uni-muenster.de)

²Zentrallaboratorium für Geochronologie, Institut für Mineralogie, Westfälische Wilhelm-Universität, Corrensstrasse 24, 481 49 Münster, Germany

Whole rock samples of Late Devonian to Early Carboniferous metaturbiditic greywackes have been analysed for its Nd isotopes to define possible sources for the sediments. The result is interpreted together with the petrography and the geochemistry of the rocks. The studied sediments are part of the so called basement of the Andes; the oldest rocks in southernmost Andean Patagonia. They are deformed and low-grade metamorphosed, due to their position in the back-stop of a Late Palaeozoic to Early Mesozoic accretionary wedge.

The petrographic framework is dominated by quartz grains. Polycrystalline lithic fragments are sparse. The cathodoluminescence characters of individual quartz grains reveal a dominance of quartz of metamorphic and plutonic origin. Volcanic quartz grains are rare. Further, signs of recycling can be seen. The geochemistry indicates that the sediments mainly had felsic source rocks. However, based on petrographic and geochemical data alone, the discrimination of the tectonic setting (passive vs. active tectonic margin) for the main sources of the metaturbidites was not satisfactory.

A first set of samples from the mainland of southern Chile have been analysed for its Nd isotopes. They show Grenvillian Nd model ages with a main interval of 1340-1490 Ma. Thus, the source rocks were part of a Precambrian crust in the Late Palaeozoic. For the model age calculation a multistage model was used, which allows for disturbance of the isotope signal at the time for deposition. The mean interval for $_{Nd}(T=sed)$ is between -6 and -4.5; further indications of a felsic, crustal origin for the sources. Further analyses will show if similar rocks from the Chilean archipelago and western Argentina have corresponding Nd signatures.

The analysed Chilean Late Devonian to Early Carboniferous metasediments have similar Nd model ages to pre-Devonian metamorphic, cratonic rocks situated in Extra-Andean Argentinian Patagonia. The sources of the Chilean turbidite deposits are suggested to be of the same origin as the Extra-Andean rocks. Thus, we suggest that the main sedimentary input came from the interior of Gondwana.

Sulfides from the lower mantle?

S. AULBACH¹, W.L. GRIFFIN^{1,2}, S.Y. O'REILLY¹ AND K. KIVI³

¹ GEMOC ARC National Key Centre, Macquarie University, NSW 2109, Australia (saulb001@laurel.ocs.mq.edu.au)

² CSIRO Exploration and Mining, N. Ryde, NSW 2113, Australia

³ Kennecott Canada Exploration Inc., 1300 Walsh Street, Thunder Bay, ONT. P7E 4X4, Canada

The Lac de Gras (Slave Craton, Canada) kimberlites sampled monosulfide solid solution (mss), Ni-Co-rich sulfides ($(Ni,Fe)_{3-x}S_2$) and Fe metal included in peridotitic minerals. This inclusion suite is unusual because: (1) $(Ni,Fe)_{3-x}S_2$ have low Ni/Co (mean 6.5 versus 21 for chondrite); (2) all $(Ni,Fe)_{3-x}S_2$, a subgroup of the mss and the Fe metal inclusion have high mean W-contents of 1.2, 1.6 and 2.9 wt%, respectively, and high W/Mo; (3) $(Ni,Fe)_{3-x}S_2$ has lower Fe/Ni (0.2), Fe/Co (1.3) and higher metal/sulfur (1.2) than any sulfide suite world-wide.

We suggest the following three steps for the formation of both sulfides and metal: (1) low Ni/Co was acquired by equilibration of a metal-rich sulfide melt with silicate melt at mid-mantle pressure where $D_{Co}^{metal\ melt/silicate\ melt}$ becomes $> D_{Ni}^{metal\ melt/silicate\ melt}$ (Li and Agee, 2001); (2) high $D_W^{metal\ melt/Mg-wüstite}$ relative to $D_{Mo}^{metal\ melt/Mg-wüstite}$ and $D_W^{metal\ melt/silicate\ melt}$ (Ohtani et al., 1997) suggests high W contents and W/Mo were acquired by percolation of the metal-rich sulfide melt through the lower mantle; (3) cooling led to exsolution of this melt into S-rich and S-poor melts, with partitioning of Ni and Co into the S-rich melt, and depletion in the S-poor melt (Ballhaus and Ellis, 1996). The S-rich melt precipitated nickeliferous mss. The residual liquid became progressively depleted in S, and enriched in Ni and Co, until melt of the composition $(Ni,Fe)_{3-x}S_2$ was trapped. The S-poor melt precipitated Fe metal with low Ni and Co contents. This scenario is supported by strong negative Ni and Co anomalies in the Fe metal relative to elements of similar siderophile nature.

Modelling the three-step formation using distribution coefficients approximates the compositions of our samples although there are uncertainties in the formation conditions and applicability of the partitioning data. Sulfides and Fe metal from Lac de Gras may have been trapped in the lower mantle during the Earth's accretion, when dense metal-rich sulfide melts percolated the lower mantle *en route* to the core after equilibrating at the base of a deep magma ocean.

References

- Ballhaus C. and Ellis D.J. (1996), *Earth Planet Sci Lett.* **143**, 137-145
 Li J. and Agee C.B. (2001), *Geochim. Cosmochim. Acta* **65**, 1821-1832
 Ohtani E., Yurimoto H. and Seto S. (1997), *Phys. Earth. Planet. Int.* **100**, 97-114

Climatic conditions in the Eastern Mediterranean region during glacial marine isotopic stage 6

A. AYALON¹, M. BAR-MATTHEWS¹ AND A. KAUFMAN²

¹ Geological Survey of Israel, 30 Malchei Israel St. Jerusalem, 95501, Israel (Ayalon@mail.gsi.gov.il; matthews@mail.gsi.gov.il)

² Department of Environmental Sciences and Energy Research, Weizman Institute of Sciences, Rehovot 76100, Israel (Cikaufman@wisemail.weizmann.ac.il)

During glacial marine isotopic stage 6, from 165 to 135 kyr, large ice sheet covered northern Europe whereas conditions in the tropics were humid, with heavy African monsoons (Rossignol-Strick, 1995). This stage in the Eastern Mediterranean (EM) Sea includes a sapropel layer (S6) that differs from interglacial sapropels because it contains pollen and fauna assemblages typical of glacial conditions (Cheddadi and Rossignol-Strick, 1995). The accurate dating of speleothems from the EM region (Israel) enables us to accurately determine the precise ages of events during stage 6 which are of special importance because no means of obtaining such precise ages are possible in the marine environment.

The isotopic record of the speleothems shows that minimum $\delta^{18}\text{O}$ values of -6‰ occur at 180-178 kyr and of -6 to -4.5‰ occur from 156 to 142 kyr. $\delta^{13}\text{C}$ values vary between -13 and -10‰ . These low values are typical to the isotopic values of speleothems that have deposited during interglacial, rather than glacial conditions (Bar-Matthews et al., 2000), and indicate that in this part of the EM region, the rainfall amount increased dramatically, and the climate was influenced by the humid conditions that prevailed over North Africa. In between these intervals, the speleothems $\delta^{18}\text{O}$ values are higher (ca. -3‰) and more typical to those deposited during glacial conditions. This suggests that the climate was colder, but probably never as dry as during much of the last glacial as indicated by the relatively low $\delta^{13}\text{C}$ values (-11‰ to -10‰), suggesting that the dominant vegetation during the entire stage was of C3 type. Thus, climatic events during this stage seem to be coeval with the large expansion of the northern ice sheet on one hand, and with wet tropics with monsoon index maxima on the other hand.

The transition from marine isotopic glacial stage 6 into stage 5 on land in the EM region occurred in two steps. The first step towards wetter and warmer conditions lasted from 135 to 128 kyr, followed by a deluge period starting at 128 kyr and lasting 9000 years.

References

- Bar-Matthews M., Ayalon, A. and Kaufman, A., (2000), *Chem. Geol.* **169**, 145-156.
- Cheddadi R. and Rossignol-Strick M., (1995), *Paleoceanography* **10**, 291-300
- Rossignol-Strick M., (1995), *Quat. Sci. Rev.* **14**, 893-915

